

# OPTIMAL LOW-RANK APPROXIMATIONS OF BAYESIAN LINEAR INVERSE PROBLEMS

ALESSIO SPANTINI\*, ANTTI SOLONEN\*<sup>§</sup>, TIANGANG CUI\*, JAMES MARTIN<sup>†</sup>, LUIS TENORIO<sup>‡</sup>, AND YOUSSEF MARZOUK\*

**Abstract.** In the Bayesian approach to inverse problems, data are often informative, relative to the prior, only on a low-dimensional subspace of the parameter space. Significant computational savings can be achieved by using this subspace to characterize and approximate the posterior distribution of the parameters. We first investigate approximation of the posterior covariance matrix as a low-rank update of the prior covariance matrix. We prove optimality of a particular update, based on the leading eigendirections of the matrix pencil defined by the Hessian of the log-likelihood and the prior precision, for a broad class of loss functions. This class includes the Förstner metric for symmetric positive definite matrices, as well as the Kullback-Leibler divergence and the Hellinger distance between the associated distributions. We also propose two fast approximations of the posterior mean and prove their optimality with respect to a weighted Bayes risk under squared-error loss. These approximations are particularly useful when repeated posterior mean evaluations are required for multiple data sets. We demonstrate our theoretical results with several numerical examples, including high-dimensional X-ray tomography and an inverse heat conduction problem. In both of these examples, the intrinsic low-dimensional structure of the inference problem can be exploited while producing results that are essentially indistinguishable from solutions computed in the full space.

**Key words.** inverse problems, Bayesian inference, low-rank approximation, covariance approximation, Förstner-Moonen metric, posterior mean approximation, Bayes risk, optimality

**1. Introduction.** In the Bayesian approach to inverse problems, the parameters of interest are treated as random variables, endowed with a prior probability distribution that encodes information available before any data are observed. Observations are modeled by their joint probability distribution conditioned on the parameters of interest, which defines the likelihood function and incorporates the forward model and a stochastic description of measurement or model errors. The prior and likelihood then combine to yield a probability distribution for the parameters conditioned on the observations, i.e., the posterior distribution. While this formulation is quite general, essential features of inverse problems bring additional structure to the Bayesian update. The prior distribution often encodes some kind of smoothness or correlation among the inversion parameters; observations typically are finite, few in number, and corrupted by noise; and the observations are indirect, related to the inversion parameters by the action of a forward operator that destroys some information. A key consequence of these features is that the data may be informative, relative to the prior, only on a *low-dimensional subspace* of the entire parameter space. Identifying and exploiting this subspace—to design approximations of the posterior distribution and related Bayes estimators—can lead to substantial computational savings.

In this paper we investigate approximation methods for finite-dimensional Bayesian linear inverse problems with Gaussian measurement and prior distributions. We characterize approximations of the posterior distribution that are structure-exploiting and that are *optimal* in a sense to be defined below. Since the posterior distribution is Gaussian, it is completely determined by its mean and covariance. We therefore focus on approximations of these posterior characteristics. Optimal approximations will reduce computation and storage requirements for high-dimensional inverse problems, and will also enable fast computation of the posterior mean in a many-query setting.

We consider approximations of the posterior covariance matrix in the form of low-rank negative updates of the prior covariance matrix. This class of approximations exploits the structure of the prior-to-posterior update; the challenge is to find an *optimal* update within this class. We will

\*Department of Aeronautics and Astronautics, Massachusetts Institute of Technology, Cambridge, MA 02139, USA, {spantini, solonen, tcui, ymarz}@mit.edu.

<sup>†</sup>Institute for Computational Engineering and Sciences, University of Texas at Austin, Austin, TX 78712 USA, jmartin@ices.utexas.edu.

<sup>‡</sup>Applied Mathematics and Statistics, Colorado School of Mines, Golden, CO 80401, USA, ltenorio@mines.edu.

<sup>§</sup>Lappeenranta University of Technology, Department of Mathematics and Physics, 53851 Lappeenranta, Finland.

argue that a suitable loss function with which to define optimality is the Förstner metric [13] for symmetric positive definite matrices, and will show that this metric generalizes to a broader class of loss functions that emphasize relative differences in covariance. We will derive the optimal low-rank update for this entire class of loss functions. In particular, we will show that the prior covariance matrix should be updated along the leading generalized eigenvectors of the pencil defined by the Hessian of the log-likelihood and the prior precision matrix. If we assume exact knowledge of the posterior mean, then our results extend to optimality statements between distributions (e.g., optimality in Kullback-Leibler divergence and in Hellinger distance). The form of this low-rank update of the prior is not new [2, 5, 12, 27], but previous work has not shown whether—and if so, in exactly what sense—it yields optimal approximations of the posterior. A key contribution of this paper is to establish and explain this optimality.

One often justifies the assumption that the posterior mean is exactly known by arguing that it easily can be computed as the solution of a regularized least-squares problem, e.g., through the application of large-scale matrix-free algorithms [1]; indeed, evaluation of the posterior mean to machine precision is now feasible even for million-dimensional parameter spaces [2]. If, however, one needs multiple evaluations of the posterior mean for different realizations of the data (e.g., in an online inference context), then solving a linear system to determine the posterior mean may not be the most efficient strategy. A second goal of our paper is to address this problem. We will propose two computationally efficient approximations of the posterior mean based on: (i) evaluating a low-rank affine function of the data; or (ii) using a low-rank update of the prior covariance matrix in the exact formula for the posterior mean. The optimal approximation in each case is defined as the minimizer of the Bayes risk for a squared-error loss defined by the posterior precision matrix. We provide explicit formulas for these optimal approximations and show that they can be computed by exploiting the optimal posterior covariance approximation described above. Thus, given a new set of data, computing an optimal approximation of the posterior mean becomes a computationally trivial task.

Low-rank approximations of the posterior mean that minimize the Bayes risk for squared-error loss under the standard Euclidean norm have been proposed in [8, 9]. Here, we instead develop analytical results for squared-error loss weighted by the posterior precision matrix. This choice of norm reflects the idea that approximation errors in directions of low posterior variance should be penalized more strongly than errors in high-variance directions, as we do not want the approximate posterior mean to fall outside the bulk of the posterior probability distribution. Remarkably, in this case, the optimal approximation only requires the leading eigenvectors and eigenvalues of a single eigenvalue problem. This is the same eigenvalue problem we solve to obtain an optimal approximation of the posterior covariance, and thus we can efficiently obtain both approximations at the same time.

While the efficient solution of large-scale linear-Gaussian Bayesian inverse problems is of standalone interest [12], optimal approximations of Gaussian posteriors are also a building block for the solution of nonlinear Bayesian inverse problems. For example, the stochastic Newton Markov chain Monte Carlo (MCMC) method [27] uses Gaussian proposals derived from local linearizations of a nonlinear forward model; the parameters of each Gaussian proposal are computed using the optimal approximations analyzed in this paper. To tackle even larger nonlinear inverse problems, [2] uses a Laplace approximation of the posterior distribution wherein the Hessian at the mode of the log-posterior density is itself approximated using the present approach. Similarly, approximations of local Gaussians can facilitate the construction of a nonstationary Gaussian process whose mean directly approximates the posterior density [4]. Alternatively, [11] combines data-informed directions derived from local linearizations of the forward model—a direct extension of the posterior covariance approximations described in the present work—to create a global *data-informed subspace*. A computationally efficient approximation of the posterior distribution is then obtained by restricting MCMC to this subspace and treating complementary directions analytically. Moving from the finite to the infinite-dimensional setting, the same global data-informed subspace is used to drive efficient

dimension-independent posterior sampling for inverse problems in [10].

Earlier work on dimension reduction for Bayesian inverse problems used the Karhunen-Loève expansion of the prior distribution [28, 22] to describe the parameters of interest. To reduce dimension, this expansion is truncated; this step renders both the prior and posterior distributions singular—i.e., collapsed onto the prior mean—in the neglected directions. Avoiding large truncation errors then requires that the prior distribution impose significant smoothness on the parameters, so that the spectrum of the prior covariance kernel decays quickly. In practice, this requirement restricts the choice of priors. Moreover, this approach relies entirely on properties of the prior distribution and does not incorporate the influence of the forward operator or the observational errors. Alternatively, [24] constructs a reduced basis for the parameter space via greedy model-constrained sampling, but this approach can also fail to capture posterior variability in directions uninformed by the data. Both of these earlier approaches seek reduction in the overall description of the parameters. This notion differs fundamentally from the dimension reduction technique advocated in this paper, where low-dimensional structure is sought in the *change* from prior to posterior.

The rest of this paper is organized as follows. In Section 2 we introduce the posterior covariance approximation problem and derive the optimal prior-to-posterior update with respect to a broad class of loss functions. The structure of the optimal posterior covariance matrix approximation is examined in Section 3. Several interpretations are given in this section, including an equivalent reformulation of the covariance approximation problem as an optimal *projection* of the likelihood function onto a lower dimensional subspace. In Section 4 we characterize optimal approximations of the posterior mean. In Section 5 we provide several numerical examples. Section 6 offers concluding remarks. Appendix A collects proofs of many of the theorems offered in the preceding sections, along with additional technical results.

**2. Optimal approximation of the posterior covariance.** Consider the Bayesian linear model defined by a Gaussian likelihood and a Gaussian prior with a non-singular covariance matrix  $\Gamma_{\text{pr}} \succ 0$  and, without loss of generality, zero mean:

$$y \mid x \sim \mathcal{N}(Gx, \Gamma_{\text{obs}}), \quad x \sim \mathcal{N}(0, \Gamma_{\text{pr}}). \quad (2.1)$$

It is easy to see that the posterior distribution is again Gaussian (see, e.g., [6])

$$x \mid y \sim \mathcal{N}(\mu_{\text{pos}}(y), \Gamma_{\text{pos}}),$$

with mean and covariance matrix given by

$$\mu_{\text{pos}}(y) = \Gamma_{\text{pos}} G^\top \Gamma_{\text{obs}}^{-1} y \quad \text{and} \quad \Gamma_{\text{pos}} = (H + \Gamma_{\text{pr}}^{-1})^{-1}, \quad (2.2)$$

where

$$H = G^\top \Gamma_{\text{obs}}^{-1} G \quad (2.3)$$

is the Hessian of the log-likelihood (i.e., the Fisher information matrix). Since the posterior is Gaussian, the posterior mean coincides with the posterior mode:  $\mu_{\text{pos}}(y) = \arg \max_x \pi_{\text{pos}}(x; y)$ , where  $\pi_{\text{pos}}$  is the posterior density.

**2.1. Approximation class.** We will seek an approximation  $\hat{\Gamma}_{\text{pos}}$  of the posterior covariance matrix that is optimal in a class of matrices to be defined shortly. As we can see from (2.2), the posterior precision matrix  $\Gamma_{\text{pos}}^{-1}$  is a non-negative update of the prior precision matrix  $\Gamma_{\text{pr}}^{-1}$ :  $\Gamma_{\text{pos}}^{-1} = \Gamma_{\text{pr}}^{-1} + JJ^\top$ , where  $JJ^\top = H$ . Similarly, using Woodbury's identity we can write  $\Gamma_{\text{pos}}$  as a non-positive update of  $\Gamma_{\text{pr}}$ :

$$\Gamma_{\text{pos}} = \Gamma_{\text{pr}} - KK^\top,$$

where

$$KK^\top = \Gamma_{\text{pr}} G^\top \Gamma_y^{-1} G \Gamma_{\text{pr}}$$

and  $\Gamma_y = \Gamma_{\text{obs}} + G \Gamma_{\text{pr}} G^\top$  is the covariance of the marginal distribution of  $y$ . This update of  $\Gamma_{\text{pr}}$  is negative semidefinite because the data add information; they cannot increase the prior variance in any direction. Moreover, the update is usually low rank for exactly the reasons described in the introduction: there are directions in the parameter space along which the data are not very informative, relative to the prior. For instance,  $H$  might have a quickly decaying spectrum [3]. Note, however, that  $\Gamma_{\text{pos}}$  itself might *not* be low-rank. Low-rank structure, if any, lies in the update of  $\Gamma_{\text{pr}}$  that yields  $\Gamma_{\text{pos}}$ . Hence, a natural class of matrices for approximating  $\Gamma_{\text{pos}}$  is the set of negative semi-definite updates of  $\Gamma_{\text{pr}}$ , with a fixed maximum rank, that lead to positive definite matrices:

$$\mathcal{M}_r = \{ \Gamma_{\text{pr}} - KK^\top \succ 0 : \text{rank}(K) \leq r \}. \quad (2.4)$$

This class of approximations of the posterior covariance takes advantage of the structure of the prior-to-posterior update.

**2.2. Loss functions.** Optimality statements regarding the approximation of a covariance matrix require an appropriate notion of distance between symmetric positive definite (SPD) matrices. We shall use the metric introduced by Förstner and Moonen [13], which is derived from a canonical invariant metric on the cone of real SPD matrices and is defined as follows: the Förstner distance  $d_{\mathcal{F}}(A, B)$  between a pair of SPD matrices  $A$  and  $B$  is given by

$$d_{\mathcal{F}}^2(A, B) = \text{tr} \left[ \ln^2(A^{-1/2} B A^{-1/2}) \right] = \sum_i \ln^2(\sigma_i),$$

where  $(\sigma_i)$  are the generalized eigenvalues of the pencil  $(A, B)$ . The Förstner metric satisfies the following important invariance properties:

$$d_{\mathcal{F}}(A, B) = d_{\mathcal{F}}(A^{-1}, B^{-1}), \quad d_{\mathcal{F}}(A, B) = d_{\mathcal{F}}(MAM^\top, MBM^\top) \quad (2.5)$$

for any nonsingular matrix  $M$ . Moreover,  $d_{\mathcal{F}}$  treats under- and over-approximations similarly in the sense that  $d_{\mathcal{F}}(\Gamma_{\text{pos}}, \alpha \hat{\Gamma}_{\text{pos}}) \rightarrow \infty$  as  $\alpha \rightarrow 0$  and as  $\alpha \rightarrow \infty$ .<sup>1</sup> Note that the metric induced by the Frobenius norm does not satisfy any of the aforementioned invariance properties. In addition, it penalizes under- and over-estimation differently.

We will show that our posterior covariance matrix approximation is optimal not only in terms of the Förstner metric, but also in terms of the following more general class  $\mathcal{L}$  of loss functions for SPD matrices.

**DEFINITION 2.1 (Loss functions).** *The class  $\mathcal{L}$  is defined as the collection of functions of the form*

$$L(A, B) = \sum_{i=1}^n f(\sigma_i), \quad (2.6)$$

where  $A$  and  $B$  are SPD matrices,  $(\sigma_i)$  are the generalized eigenvalues of the pencil  $(A, B)$ , and

$$f \in \mathcal{U} = \{ g \in \mathcal{C}^1(\mathbb{R}_+) : g'(x)(1-x) < 0 \text{ for } x \neq 1, \text{ and } \lim_{x \rightarrow \infty} g(x) = \infty \}. \quad (2.7)$$

<sup>1</sup>This behavior is shared by Stein's loss function, which has been proposed to assess estimates of a covariance matrix [19]. Stein's loss function is just the Kullback-Leibler distance between two Gaussian distributions with the same mean (see (A.10)), but it is not a metric for SPD matrices.

Elements of  $\mathcal{U}$  are essentially differentiable real-valued functions defined on the positive axis that are decreasing for  $x < 1$  and increasing for  $x > 1$ , tending to infinity as  $x \rightarrow \infty$ . The squared Förstner metric belongs to the class of loss functions defined above in (2.6), whereas the distance induced by the Frobenius norm does not.

Lemma 2.2, whose proof can be found in Appendix A, justifies the importance of the class  $\mathcal{L}$ . In particular, it shows that optimality of the covariance matrix approximation with respect to any loss function in  $\mathcal{L}$  leads to an optimal approximation of the posterior distribution using a Gaussian with the same mean in terms of other familiar criteria used to compare probability measures, such as the Hellinger distance and the Kullback-Leibler (K-L) divergence [29]. More precisely, we have the following result:

**LEMMA 2.2** (Equivalence of approximations). *If  $L \in \mathcal{L}$ , then a matrix  $\hat{\Gamma}_{\text{pos}} \in \mathcal{M}_r$  minimizes the Hellinger distance and the K-L divergence between  $\mathcal{N}(\mu_{\text{pos}}(y), \Gamma_{\text{pos}})$  and the approximation  $\mathcal{N}(\mu_{\text{pos}}(y), \hat{\Gamma}_{\text{pos}})$  iff it minimizes  $L(\Gamma_{\text{pos}}, \hat{\Gamma}_{\text{pos}})$ .*

**REMARK 1.** We note that neither the Hellinger distance nor the K-L divergence between the distributions  $\mathcal{N}(\mu_{\text{pos}}(y), \Gamma_{\text{pos}})$  and  $\mathcal{N}(\mu_{\text{pos}}(y), \hat{\Gamma}_{\text{pos}})$  depends on the data  $y$ . Optimality in distribution does not necessarily hold when the posterior means are different.

**2.3. Optimality results.** We are now in a position to state one of the main results of the paper. For a proof see Appendix A.

**THEOREM 2.3** (Optimal posterior covariance approximation). *Let  $S_{\text{pr}}$  be any square root<sup>2</sup> of the prior covariance matrix such that  $\Gamma_{\text{pr}} = S_{\text{pr}} S_{\text{pr}}^\top$ . Let  $(\delta_i^2, w_i)$  be the eigenvalue-eigenvector pairs of the prior-preconditioned Hessian:*

$$\hat{H} = S_{\text{pr}}^\top H S_{\text{pr}} \quad (2.8)$$

*with the ordering  $\delta_i^2 \geq \delta_{i+1}^2$ , and let  $L$  be a loss function in the class  $\mathcal{L}$  defined in (2.6). Then:*

*(i) A minimizer,  $\hat{\Gamma}_{\text{pos}}$ , of the loss  $L$  between  $\Gamma_{\text{pos}}$  and an element of  $\mathcal{M}_r$  is given by:*

$$\hat{\Gamma}_{\text{pos}} = \Gamma_{\text{pr}} - K K^\top, \quad K K^\top = \sum_{i=1}^r \delta_i^2 (1 + \delta_i^2)^{-1} \hat{w}_i \hat{w}_i^\top, \quad \hat{w}_i = S_{\text{pr}} w_i. \quad (2.9)$$

*The corresponding minimum loss is given by:*

$$L(\hat{\Gamma}_{\text{pos}}, \Gamma_{\text{pos}}) = f(1) r + \sum_{i>r} f(1/(1 + \delta_i^2)). \quad (2.10)$$

*(ii) The minimizer (2.9) is unique if the first  $r$  eigenvalues of  $\hat{H}$  are distinct.*

Theorem 2.3 provides a way to construct the best approximation of  $\Gamma_{\text{pos}}$  by matrices in  $\mathcal{M}_r$ : it is just a matter of computing the eigen-pairs corresponding to the decreasing sequence of eigenvalues of  $\hat{H}$  until a stopping criterion is satisfied. This criterion can be based on the minimum loss (2.10). Lanczos iteration or a randomized SVD are ideal matrix-free methods to solve this symmetric eigenvalue problem even for large-scale applications [2, 16]. Notice that the directions  $(\hat{w}_i)$  defining the prior-to-posterior update in (2.9) are the generalized eigenvectors of the pencil  $(H, \Gamma_{\text{pr}}^{-1})$ . These directions are orthogonal with respect to the inner product induced by the prior precision matrix, and they maximize the Rayleigh ratio

$$\hat{\mathcal{R}}(z) = \frac{z^\top H z}{z^\top \Gamma_{\text{pr}}^{-1} z}$$

---

<sup>2</sup> $S_{\text{pr}}$  can be either a non-symmetric square root (e.g., a Cholesky factor of  $\Gamma_{\text{pr}}$ ) or a symmetric square root (e.g., when the action of the prior precision on a vector is specified through an elliptic operator [25]).

over subspaces of the form  $\widehat{\mathcal{W}}_i = \text{span}^\perp(\widehat{w}_j)_{j < i}$ . Intuitively, the vectors  $\widehat{w}_i$  associated with generalized eigenvalues greater than one correspond to directions in the parameter space (or subspaces thereof) where the curvature of the log-posterior density is constrained more by the log-likelihood than by the prior.

REMARK 2. It is straightforward to obtain an expression for a non-symmetric square root of the optimal approximation of  $\Gamma_{\text{pos}}$  (2.9) as in [5]:

$$\widehat{S}_{\text{pos}} = S_{\text{pr}} \left( \sum_{i=1}^r \left[ (1 + \delta_i^2)^{-1/2} - 1 \right] w_i w_i^\top + I \right) \quad (2.11)$$

such that  $\widehat{\Gamma}_{\text{pos}} = \widehat{S}_{\text{pos}} \widehat{S}_{\text{pos}}^\top$ . This expression can be used to efficiently sample from the approximate posterior distribution  $\mathcal{N}(\mu_{\text{pos}}(y), \widehat{\Gamma}_{\text{pos}})$ .

**3. Properties of the optimal covariance approximation.** Now we discuss several implications of the optimal approximation of  $\Gamma_{\text{pos}}$  introduced in the previous section. First, we describe the relationship between this approximation and the directions of greatest relative reduction of prior variance. Then we interpret the covariance approximation as the result of projecting the likelihood function onto a “data-informed” subspace. Finally, we contrast the present approach with several other approximation strategies: using the Frobenius norm as a loss function for the covariance matrix approximation, or developing low-rank approximations based on prior or Hessian information alone.

**3.1. Interpretation of the eigendirections.** Thanks to the particular structure of loss functions in  $\mathcal{L}$ , the problem of approximating  $\Gamma_{\text{pos}}$  is equivalent to that of approximating  $\Gamma_{\text{pos}}^{-1}$ . Yet the form of the optimal approximation of  $\Gamma_{\text{pos}}^{-1}$  is important, as it explicitly describes the directions that control the ratio of posterior to prior variance. The following corollary to Theorem 2.3 characterizes these directions. The proof is in Appendix A.

COROLLARY 3.1 (Optimal posterior precision approximation). *Let  $S_{\text{pr}}$ ,  $(\delta_i^2, w_i)$ ,  $\widehat{H}$ , and  $L \in \mathcal{L}$  be defined as in Theorem 2.3. Then:*

(i) *A minimizer of  $L(B, \Gamma_{\text{pos}}^{-1})$  for*

$$B \in \mathcal{M}_r^{-1} := \{ \Gamma_{\text{pr}}^{-1} + J J^\top : \text{rank}(J) \leq r \} \quad (3.1)$$

*is given by*

$$\widehat{\Gamma}_{\text{pos}}^{-1} = \Gamma_{\text{pr}}^{-1} + U U^\top, \quad U U^\top = \sum_{i=1}^r \delta_i^2 \widetilde{w}_i \widetilde{w}_i^\top, \quad \widetilde{w}_i = S_{\text{pr}}^{-\top} w_i. \quad (3.2)$$

*The minimizer (3.2) is unique if the first  $r$  eigenvalues of  $\widehat{H}$  are distinct.*

(ii) *The optimal posterior precision matrix (3.2) is precisely the inverse of the optimal posterior covariance matrix (2.9).*

(iii) *The vectors  $\widetilde{w}_i$  are generalized eigenvectors of the pencil  $(\Gamma_{\text{pos}}, \Gamma_{\text{pr}})$ :*

$$\Gamma_{\text{pos}} \widetilde{w}_i = \frac{1}{1 + \delta_i^2} \Gamma_{\text{pr}} \widetilde{w}_i. \quad (3.3)$$

Note that the definition of the class  $\mathcal{M}_r^{-1}$  is analogous to that of  $\mathcal{M}_r$ . Indeed, Lemma A.2 in Appendix A defines a bijection between these two classes.

The vectors  $\widetilde{w}_i = S_{\text{pr}}^{-\top} w_i$  are orthogonal with respect to the inner product defined by  $\Gamma_{\text{pr}}$ . By (3.3), we also know that  $\widetilde{w}_i$  minimize the generalized Rayleigh quotient

$$\mathcal{R}(z) = \frac{z^\top \Gamma_{\text{pos}} z}{z^\top \Gamma_{\text{pr}} z} = \frac{\text{Var}(z^\top x | y)}{\text{Var}(z^\top x)} \quad (3.4)$$

over subspaces of the form  $\widetilde{\mathcal{W}}_i = \text{span}^\perp(\widetilde{w}_j)_{j < i}$ . This Rayleigh quotient is precisely the *ratio of posterior to prior variance* along a particular direction  $z$  in the parameter space. The smallest values that  $\mathcal{R}$  can take over the subspaces  $\widetilde{\mathcal{W}}_i$  are exactly the smallest generalized eigenvalues of  $(\Gamma_{\text{pos}}, \Gamma_{\text{pr}})$ . In particular, the data are most informative along the first  $r$  eigenvectors  $\widetilde{w}_i$  and, since

$$\mathcal{R}(\widetilde{w}_i) = \frac{\text{Var}(\widetilde{w}_i^\top x | y)}{\text{Var}(\widetilde{w}_i^\top x)} = \frac{1}{1 + \delta_i^2}, \quad (3.5)$$

the posterior variance is smaller than the prior variance by a factor of  $(1 + \delta_i^2)^{-1}$ . In the span of the other eigenvectors,  $(\widetilde{w}_i)_{i > r}$ , the data are not as informative. Hence,  $(\widetilde{w}_i)$  are the directions along which the ratio of posterior to prior variance is minimized. Furthermore, a simple computation shows that these directions also maximize the relative difference between prior and posterior variance normalized by the prior variance. Indeed, if the directions  $(\widetilde{w}_i)$  minimize (3.4) then they must also maximize  $1 - \mathcal{R}(z)$ , leading to:

$$1 - \mathcal{R}(\widetilde{w}_i) = \frac{\text{Var}(\widetilde{w}_i^\top x) - \text{Var}(\widetilde{w}_i^\top x | y)}{\text{Var}(\widetilde{w}_i^\top x)} = \frac{\delta_i^2}{1 + \delta_i^2}. \quad (3.6)$$

**3.2. Optimal projector.** Since the data are most informative on a subspace of the parameter space, it should be possible to reduce the *effective dimension* of the inference problem in a manner that is consistent with the posterior approximation. This is essentially the content of the following corollary, which follows by a simple computation.

**COROLLARY 3.2 (Optimal projector).** *Let  $\widehat{\Gamma}_{\text{pos}}$ ,  $S_{\text{pr}}$ , and the vectors  $(w_i)$  be defined as in Theorem 2.3. Consider the reduced forward operator  $\widehat{G}_r = G \circ P_r$ , where  $P_r$  is the oblique projector (i.e.,  $P_r^2 = P_r$ ):*

$$P_r = S_{\text{pr}} \left( \sum_{i=1}^r w_i w_i^\top \right) S_{\text{pr}}^{-1}. \quad (3.7)$$

*Then  $\widehat{\Gamma}_{\text{pos}}$  is precisely the posterior covariance matrix corresponding to the Bayesian linear model:*

$$y | x \sim \mathcal{N}(\widehat{G}_r x, \Gamma_{\text{obs}}), \quad x \sim \mathcal{N}(0, \Gamma_{\text{pr}}). \quad (3.8)$$

The projected linear Gaussian model (3.8) reveals the intrinsic dimensionality of the inference problem. The introduction of the optimal projector (3.7) is also useful in the context of dimensionality reduction for nonlinear inverse problems. In this case a particularly simple and effective approximation of the posterior density  $\pi_{\text{pos}}(x|y)$  is of the form  $\widehat{\pi}_{\text{pos}}(x|y) \propto \pi(y; P_r x) \pi_{\text{pr}}(x)$ , where  $\pi_{\text{pr}}$  is the prior density and  $\pi(y; P_r x)$  is the density corresponding to the likelihood function with parameters constrained by the projector. The range of the projector can be determined by combining locally optimal data-informed subspaces from high-density regions in the support of the posterior distribution. This approximation is the subject of a related paper [11].

Returning to the linear inverse problem, notice also that the posterior mean of the projected model (3.8) might be used as an efficient approximation of the exact posterior mean. We will show in Section 4 that this posterior mean approximation in fact minimizes the Bayes risk for a weighted squared-error loss among all low-rank linear functions of the data.

**3.3. Comparison with optimality in Frobenius norm.** Thus far our optimality results for the approximation of  $\Gamma_{\text{pos}}$  have been restricted to the class of loss functions  $\mathcal{L}$  given in Definition 2.1. However, it is interesting also to investigate optimality in the metric defined by the Frobenius norm. Given any two matrices  $A$  and  $B$  of the same size, the Frobenius distance between them is defined as  $\|A - B\|$ , where  $\|\cdot\|$  is the Frobenius norm. Note that the Frobenius distance does not exploit the



structure of the positive definite cone of symmetric matrices. The matrix  $\hat{\Gamma}_{\text{pos}} \in \mathcal{M}_r$  that minimizes the Frobenius distance from the exact posterior covariance matrix is given by:

$$\hat{\Gamma}_{\text{pos}} = \Gamma_{\text{pr}} - K K^\top, \quad K K^\top = \sum_{i=1}^r \lambda_i u_i u_i^\top, \quad (3.9)$$

where  $(u_i)$  are the directions corresponding to the  $r$  largest eigenvalues of  $\Gamma_{\text{pr}} - \Gamma_{\text{pos}}$ . This result can be very different from the optimal approximation given in Theorem 2.3. In particular, the directions  $(u_i)$  are solutions of the eigenvalue problem

$$\Gamma_{\text{pr}} G^\top \Gamma_y^{-1} G \Gamma_{\text{pr}} u = \lambda u, \quad (3.10)$$

which maximize

$$u^\top (\Gamma_{\text{pr}} - \Gamma_{\text{pos}}) u = \mathbb{V}\text{ar}(u^\top x) - \mathbb{V}\text{ar}(u^\top x \mid y). \quad (3.11)$$

That is, while optimality in the Förstner metric identifies directions that maximize the *relative* difference between prior and posterior variance, the Frobenius distance favors directions that maximize only the absolute value of this difference. There are many reasons to prefer the former. For instance, data may be informative along directions of low prior variance (perhaps due to inadequacies in prior modeling); a covariance matrix approximation that is optimal in Frobenius distance may ignore updates in these directions entirely. Also, if parameters of interest (i.e., components of  $x$ ) have differing units of measurement, relative variance reduction provides a unit-independent way of judging the quality of a posterior approximation; this notion follows naturally from the second invariance property of  $d_{\mathcal{F}}$  in (2.5). From a computational perspective, solving the eigenvalue problem (3.10) is quite expensive compared to finding an eigendecomposition of the prior-preconditioned Hessian. Finally, optimality in the Frobenius distance for an approximation of  $\Gamma_{\text{pos}}$  does not yield an optimality statement for the corresponding approximation of the posterior distribution, as shown in Lemma 2.2 for loss functions in  $\mathcal{L}$ .

**3.4. Suboptimal posterior covariance approximations.** The posterior approximation described by Theorem 2.3 uses both Hessian and prior information. It is instructive to consider approximations of the linear Bayesian inverse problem that rely only on one or the other; as we will illustrate numerically in Section 5.1, these approximations can be viewed as natural limiting cases of our approach. They are also linked to previous efforts in dimensionality reduction that propose only Hessian-based [23] or prior-based [28] reductions. In contrast with these previous efforts, here we will consider versions of Hessian- and prior-based reduction that do not discard prior information in the remaining directions. In other words, we will discuss posterior covariance approximations that remain in the form of (2.4)—i.e., updating the prior covariance only in  $r$  directions.

A Hessian-based reduction scheme updates  $\Gamma_{\text{pr}}$  in directions where the data have greatest influence in an absolute sense (i.e., not relative to the prior). This involves approximating the log-likelihood Hessian (2.3) with a low-rank decomposition as follows: let  $(s_i^2, v_i)$  be the eigenvalue-eigenvector pairs of  $H$  with the ordering  $s_i^2 \geq s_{i+1}^2$ . Then a best low-rank approximation of  $H$  in the Frobenius norm is given by:

$$H \approx \sum_{i=1}^r s_i^2 v_i v_i^\top = V_r S_r V_r^\top,$$

where  $v_i$  is the  $i$ th column of  $V_r$  and  $S_r = \text{diag}\{s_1^2, \dots, s_r^2\}$ . Using Woodbury's identity we then obtain an approximation of  $\Gamma_{\text{pos}}$  as a low-rank negative semidefinite update of  $\Gamma_{\text{pr}}$ :

$$\Gamma_{\text{pos}} \approx (V_r S_r V_r^\top + \Gamma_{\text{pr}}^{-1})^{-1} = \Gamma_{\text{pr}} - \Gamma_{\text{pr}} V_r (S_r^{-1} + V_r^\top \Gamma_{\text{pr}} V_r)^{-1} V_r^\top \Gamma_{\text{pr}}. \quad (3.12)$$



This approximation of the posterior covariance matrix belongs to the class  $\mathcal{M}_r$ . Thus, Hessian-based reduction is in general suboptimal when compared to the optimal approximation defined in Theorem 2.3. Note that an equivalent way to obtain (3.12) is to use a reduced forward operator of the form  $\hat{G} = G \circ V_r V_r^\top$ , which is the composition of the original forward operator with a projector onto the leading eigenspace of  $H$ . In general, the projector  $P_r = V_r V_r^\top$  is different from the optimal projector defined in Corollary 3.2 and is thus suboptimal.

To achieve prior-based reduction, on the other hand, we restrict the Bayesian inference problem to directions in the parameter space that explain most of the prior variance. More precisely, we look for a rank- $r$  orthogonal projector  $P_r$  that minimizes the mean squared-error defined as:

$$\mathcal{E}(P_r) = \mathbb{E}(\|x - P_r x\|^2), \quad (3.13)$$

where the expectation is taken over the prior distribution (assumed to have zero mean) and  $\|\cdot\|$  is the standard Euclidean norm [18]. Let  $(t_i^2, u_i)$  be the eigenvalue-eigenvector pairs of  $\Gamma_{\text{pr}}$  ordered as  $t_i^2 \geq t_{i+1}^2$ . Then a minimizer of (3.13) is given by the projector  $P_r$  onto the leading eigenspace of  $\Gamma_{\text{pr}}$ :

$$P_r = \sum_{i=1}^r u_i u_i^\top = U_r U_r^\top,$$

where  $u_i$  is the  $i$ th column of  $U_r$ . The actual approximation of the linear inverse problem consists of using the projected forward operator,  $\hat{G} = G \circ U_r U_r^\top$ . By direct comparison with the optimal projector defined in Corollary 3.2, we see that the prior-based reduction is suboptimal in general. Also in this case, the posterior covariance matrix of the projected Gaussian model can be written as a negative semidefinite update of  $\Gamma_{\text{pr}}$ :

$$\Gamma_{\text{pos}} \approx \Gamma_{\text{pr}} - U_r T_r [(U_r^\top H U_r)^{-1} + T_r]^{-1} T_r U_r^\top,$$

where  $T_r = \text{diag}\{t_1^2, \dots, t_r^2\}$ . The double matrix inversion makes this low-rank update computationally challenging to implement. It is also not optimal, as shown in Theorem 2.3.

To summarize, both the Hessian and the prior-based dimensionality reduction techniques are suboptimal. These methods do not take into account the interactions between the dominant directions of  $H$  and those of  $\Gamma_{\text{pr}}$ , and the relative importance of these quantities. This is a key feature of the optimal covariance approximation described in Theorem 2.3. Section 5.1 will illustrate conditions under which these interactions become essential.

**4. Optimal approximation of the posterior mean.** In this section, we will develop and characterize fast approximations of the posterior mean that can be used, for instance, to accelerate repeated inversion with multiple data sets. For the Bayesian linear model defined in (2.1), the posterior mode is equal to the posterior mean,  $\mu_{\text{pos}}(y) = \mathbb{E}(x|y)$ , which is the minimizer of the Bayes risk for squared-error loss [20, 26]. We first review this idea and establish some basic notation. Let  $S$  be an SPD matrix and let

$$L(\delta(y), x) = (x - \delta(y))^\top S (x - \delta(y)) = \|x - \delta(y)\|_S^2$$

be the loss incurred by the estimator  $\delta(y)$  of  $x$ . The Bayes risk  $R(\delta(y), x)$  of  $\delta(y)$  is defined as the average loss over the joint distribution of  $x$  and  $y$  [6, 20]:  $R(\delta(y), x) = \mathbb{E}(L(\delta(y), x))$ . Since

$$R(\delta(y), x) = \mathbb{E}(\|\delta(y) - \mu_{\text{pos}}(y)\|_S^2) + \mathbb{E}(\|\mu_{\text{pos}}(y) - x\|_S^2), \quad (4.1)$$

it follows that  $\delta(y) = \mu_{\text{pos}}(y)$  minimizes the Bayes risk over all estimators of  $x$ .

To study approximations of  $\mu_{\text{pos}}(y)$ , we use the squared-error loss function defined by the Mahalanobis distance [7] induced by  $\Gamma_{\text{pos}}^{-1}$ :  $L(\delta(y), x) = \|\delta(y) - x\|_{\Gamma_{\text{pos}}^{-1}}^2$ . This loss function accounts for

the geometry induced by the posterior measure on the parameter space, penalizing errors in the approximation of  $\mu_{\text{pos}}(y)$  more strongly in directions of lower posterior variance.

Under the assumption of zero prior mean,  $\mu_{\text{pos}}(y)$  is a linear function of the data. Hence we seek approximations of  $\mu_{\text{pos}}(y)$  of the form  $Ay$ , where  $A$  is a matrix in a class to be defined. Our goal is to obtain fast posterior mean approximations that can be applied repeatedly to multiple realizations of  $y$ . We will thus consider two classes of approximation matrices:

$$\mathcal{A}_r := \{A : \text{rank}(A) \leq r\} \quad \text{and} \quad \hat{\mathcal{A}}_r := \{A = (\Gamma_{\text{pr}} - B) G^\top \Gamma_{\text{obs}}^{-1} : \text{rank}(B) \leq r\}. \quad (4.2)$$

The class  $\mathcal{A}_r$  consists of low-rank matrices; it is standard in the statistics literature [18]. The class  $\hat{\mathcal{A}}_r$ , on the other hand, can be understood via comparison with (2.2); it simply replaces  $\Gamma_{\text{pos}}$  with a low-rank negative semidefinite update of  $\Gamma_{\text{pr}}$ . We shall henceforth use  $\mathcal{A}$  to denote either of the two classes above.

Let  $R_{\mathcal{A}}(Ay, x)$  be the Bayes risk of  $Ay$  subject to  $A \in \mathcal{A}$ . We may now restate our goal as: find  $A^* \in \mathcal{A}$  that minimizes the Bayes risk  $R_{\mathcal{A}}(Ay, x)$ . That is, find

$$R_{\mathcal{A}}(A^*y, x) = \min_{A \in \mathcal{A}} \mathbb{E}(\|Ay - x\|_{\Gamma_{\text{pos}}^{-1}}^2). \quad (4.3)$$

The following two theorems show that for either class of approximation matrices,  $\mathcal{A}_r$  or  $\hat{\mathcal{A}}_r$ , this problem admits a particularly simple analytical solution that exploits the structure of the optimal approximation of  $\Gamma_{\text{pos}}$ . The proofs of the theorems rely on a result by Friedman [14], and are given in Appendix A. We also use the fact that  $\mathbb{E}(\|\mu_{\text{pos}}(y) - x\|_{\Gamma_{\text{pos}}^{-1}}^2) = \ell$ , where  $\ell$  is the dimension of the parameter space.

**THEOREM 4.1.** *Let  $S_{\text{pr}}$  and  $S_{\text{obs}}$  be square roots of  $\Gamma_{\text{pr}}$  and  $\Gamma_{\text{obs}}$ , respectively, such that  $\Gamma = S S^\top$ . Let  $V D W^\top$  be an SVD of  $S_{\hat{H}}^\top = S_{\text{obs}}^{-1} G S_{\text{pr}}$ , where  $D = \text{diag}\{\delta_i\}$  with  $\delta_i \geq \delta_{i+1}$ . Then:*

(i) *A solution of (4.3) for  $A \in \mathcal{A}_r$  is given by:*

$$A^* = S_{\text{pr}} \left( \sum_{i=1}^r \frac{\delta_i}{1 + \delta_i^2} w_i v_i^\top \right) S_{\text{obs}}^{-1}, \quad (4.4)$$

*where  $(w_i)$  and  $(v_i)$  are, respectively, the columns of  $W$  and  $V$ .*

(ii) *The corresponding minimum Bayes risk over  $\mathcal{A}_r$  is given by:*

$$R_{\mathcal{A}_r}(A^*y, x) = \mathbb{E}(\|A^*y - \mu_{\text{pos}}(y)\|_{\Gamma_{\text{pos}}^{-1}}^2) + \mathbb{E}(\|\mu_{\text{pos}}(y) - x\|_{\Gamma_{\text{pos}}^{-1}}^2) = \sum_{i>r} \delta_i^2 + \ell. \quad (4.5)$$

Notice that the rank- $r$  posterior mean approximation given by Theorem 4.1 coincides with the posterior mean of the projected linear Gaussian model defined in (3.8). The directions  $(w_i)$  are just the eigenvectors of  $\hat{H}$  that were already computed for an optimal approximation of  $\Gamma_{\text{pos}}$ . The simple relation between left and right singular vectors of a non-symmetric matrix, in our case  $S_{\hat{H}}^\top = S_{\text{pr}}^\top G^\top S_{\text{obs}}^{-1}$ , allows for an efficient computation of the corresponding directions  $(v_i)$  [15]. Applying this approximation to a new realization of the data then requires only a *low-rank* matrix-vector product, a computationally trivial task.

**THEOREM 4.2.** *Let  $\hat{\Gamma}_{\text{pos}} \in \mathcal{M}_r$  be the optimal approximation of  $\Gamma_{\text{pos}}$  defined in Theorem 2.3. Then:*

(i) *A solution of (4.3) for  $A \in \hat{\mathcal{A}}_r$  is given by:*

$$\hat{A}^* = \hat{\Gamma}_{\text{pos}} G^\top \Gamma_{\text{obs}}^{-1}. \quad (4.6)$$

(ii) The corresponding minimum Bayes risk over  $\hat{\mathcal{A}}_r$  is given by:

$$R_{\hat{\mathcal{A}}_r}(\hat{A}^*y, x) = \mathbb{E} \left( \left\| \hat{A}^*y - \mu_{\text{pos}}(y) \right\|_{\Gamma_{\text{pos}}^{-1}}^2 \right) + \mathbb{E} \left( \left\| \mu_{\text{pos}}(y) - x \right\|_{\Gamma_{\text{pos}}^{-1}}^2 \right) = \sum_{i>r} \delta_i^6 + \ell. \quad (4.7)$$

For the estimator described by Theorem 4.2, once the optimal approximation of  $\Gamma_{\text{pos}}$  is computed, the cost of approximating  $\mu_{\text{pos}}(y)$  for a new realization of  $y$  is dominated by the adjoint and prior solves needed to apply  $G^\top$  and  $\Gamma_{\text{pr}}$ , respectively. Combining the optimal approximations of  $\mu_{\text{pos}}(y)$  and  $\Gamma_{\text{pos}}$  given by Theorems 4.2 and 2.3, respectively, yields a complete approximation of the Gaussian posterior distribution. This is precisely the approximation adopted by the stochastic Newton MCMC method [27] to describe the Gaussian proposal distribution obtained from a local linearization of the forward operator of a nonlinear Bayesian inverse problem. Our results support the algorithmic choice of [27] with precise optimality statements.

It is worth noting that the two optimal Bayes risks, (4.5) and (4.7), depend on the parameter  $r$  that defines the dimension of the corresponding approximation classes  $\mathcal{A}_r$  and  $\hat{\mathcal{A}}_r$ . In the former case,  $r$  is the rank of the optimal matrix that defines the approximation. In the latter case,  $r$  is the rank of a negative update of  $\Gamma_{\text{pr}}$  that yields the posterior covariance matrix approximation. We shall thus refer to the estimator given by Theorem 4.1 as the low-rank approximation and to the estimator given by Theorem 4.2 as the low-rank *update* approximation. In both cases, we shall refer to  $r$  as the order of the approximation. A posterior mean approximation of order  $r$  will be called *under-resolved* if more than  $r$  eigenvalues of the prior-preconditioned Hessian  $\hat{H}$  are greater than one. If this is the case, then using the low-rank update approximation is not appropriate because the associated Bayes risk includes high-order powers of eigenvalues of  $\hat{H}$  that are greater than one. Thus, under-resolved approximations tend to be more accurate when using the low-rank approximation. As we will show in Section 5, this estimator is also less expensive to compute than its counterpart in Theorem 4.2. If, on the other hand, fewer than  $r$  eigenvalues of  $\hat{H}$  are greater than one, then the optimal low-rank *update* estimator will have better performance than the optimal low-rank estimator in the following statistical sense:

$$R_{\mathcal{A}_r}(A^*y, x) - R_{\hat{\mathcal{A}}_r}(\hat{A}^*y, x) = \sum_{i>r} \delta_i^2 (1 + \delta_i^2) (1 - \delta_i^2) > 0.$$

---

**Algorithm 1** Optimal *low-rank* approximation of the posterior mean

---

INPUT: square roots  $S_{\text{pr}}$  and  $S_{\text{obs}}$  of the prior and noise covariances; forward model  $G$ ; approximation order  $r \in \mathbb{N}$

OUTPUT: approximate posterior mean  $\mu_{\text{pos}}^{(r)}(y)$

- 1: Find the  $r$  leading singular triples  $(\delta_i, v_i, w_i)$  of  $S_{\text{obs}}^{-1} G S_{\text{pr}} = \sum_i \delta_i v_i w_i^\top$  (e.g., via SVD).
  - 2: For each new realization of the data  $y$ , compute  $\mu_{\text{pos}}^{(r)}(y) = S_{\text{pr}} \left( \sum_{i=1}^r \delta_i (1 + \delta_i^2)^{-1} w_i v_i^\top \right) S_{\text{obs}}^{-1} y$ .
- 

---

**Algorithm 2** Optimal *low-rank update* approximation of the posterior mean

---

INPUT: forward and adjoint models  $G$ ,  $G^\top$ ; prior and noise precisions  $\Gamma_{\text{pr}}^{-1}$ ,  $\Gamma_{\text{obs}}^{-1}$ ; approximation order  $r \in \mathbb{N}$

OUTPUT: approximate posterior mean  $\hat{\mu}_{\text{pos}}^{(r)}(y)$

- 1: Obtain  $\hat{\Gamma}_{\text{pos}}$  as described in Theorem 2.3.
  - 2: For each new realization of the data  $y$ , compute  $\hat{\mu}_{\text{pos}}^{(r)}(y) = \hat{\Gamma}_{\text{pos}} G^\top \Gamma_{\text{obs}}^{-1} y$ .
- 

**5. Numerical examples.** Now we provide several numerical examples to illustrate the theory developed in the preceding sections. We start with a synthetic example to demonstrate various posterior covariance matrix approximations, and continue with two more realistic linear inverse problems where we also study posterior mean approximations.

**5.1. Example 1: Hessian and prior with controlled spectra.** We begin by investigating the approximation of  $\Gamma_{\text{pos}}$  as a negative semidefinite update of  $\Gamma_{\text{pr}}$ . We compare the optimal approximation obtained in Theorem 2.3 with the Hessian- and prior-based reduction schemes discussed in Section 3.4. The idea is to reveal differences between these approximations by exploring regimes where the data have differing impacts on the prior information. Since the directions defining the optimal update are the generalized eigenvectors of the pencil  $(H, \Gamma_{\text{pr}}^{-1})$ , we shall also refer to this update as the *generalized* approximation.

To compare the three approximation schemes, we start with a simple example employing diagonal Hessian and prior covariance matrices:  $G = I$ ,  $\Gamma_{\text{obs}} = \text{diag}\{\sigma_i^2\}$ , and  $\Gamma_{\text{pr}} = \text{diag}\{\lambda_i^2\}$ . Since the forward operator  $G$  is the identity, this problem can (loosely) be thought of as denoising a signal  $x$ . In this case  $H = \Gamma_{\text{obs}}^{-1}$  and  $\Gamma_{\text{pos}} = \text{diag}\{\lambda_i^2 \sigma_i^2 / (\sigma_i^2 + \lambda_i^2)\}$ . The ratios of posterior to prior variance in the canonical directions ( $e_i$ ) are

$$\frac{\text{Var}(e_i^\top x \mid y)}{\text{Var}(e_i^\top x)} = \frac{1}{1 + \lambda_i^2 / \sigma_i^2}.$$

We note that if the observation variances  $\sigma_i^2$  are constant,  $\sigma_i = \sigma$ , then the directions of greatest variance reduction are those corresponding to the largest prior variance. Hence the prior distribution alone determines the most informed directions, and the prior-based reduction is as effective as the generalized one. On the other hand, if the prior variances  $\lambda_i^2$  are constant,  $\lambda_i = \lambda$ , but the  $\sigma_i$  vary, then the directions of highest variance reduction are those corresponding to the smallest noise variance. Now the noise distribution alone determines the most important directions, and Hessian-based reduction is as effective as the generalized one. In the case of more general spectra, the important directions depend on the ratios  $\lambda_i^2 / \sigma_i^2$  and thus one has to use the information provided by both the noise and prior distributions. This happens naturally when using the generalized reduction.

We now generalize this simple case by moving to full matrices  $H$  and  $\Gamma_{\text{pr}}$  with a variety of prescribed spectra. We assume that  $H$  and  $\Gamma_{\text{pr}}$  have SVDs of the form  $H = U\Lambda U^\top$  and  $\Gamma_{\text{pr}} = V\tilde{\Lambda}V^\top$ , where  $\Lambda = \text{diag}\{\lambda_1, \dots, \lambda_n\}$  and  $\tilde{\Lambda} = \text{diag}\{\tilde{\lambda}_1, \dots, \tilde{\lambda}_n\}$  with

$$\lambda_k = \lambda_0 / k^\alpha + \tau \quad \text{and} \quad \tilde{\lambda}_k = \tilde{\lambda}_0 / k^{\tilde{\alpha}} + \tilde{\tau}.$$

To consider many different cases, the orthogonal matrices  $U$  and  $V$  are randomly and independently generated uniformly over the orthogonal group [30], leading to different realizations of  $H$  and  $\Gamma_{\text{pr}}$ . In particular,  $U$  and  $V$  are computed with a  $QR$  decomposition of a square matrix of independent standard Gaussian entries using a Gram-Schmidt orthogonalization. (In this case, the standard Householder reflections cannot be used.)

Figure 5.1 summarizes the results of the first experiment. The top row shows the prescribed spectra of  $H^{-1}$  (red) and  $\Gamma_{\text{pr}}$  (blue). Parameters describing the eigenvalues of  $\Gamma_{\text{pr}}$  are fixed to  $\tilde{\lambda}_0 = 1$ ,  $\tilde{\alpha} = 2$ , and  $\tilde{\tau} = 10^{-6}$ . The corresponding parameters for  $H$  are given by  $\lambda_0 = 500$  and  $\tau = 10^{-6}$  with  $\alpha = 0.345$  (left),  $\alpha = 0.690$  (middle), and  $\alpha = 1.724$  (right). Thus, moving from the leftmost column to the rightmost column, the data become increasingly less informative. The second row in the figure shows the Förstner distance between  $\Gamma_{\text{pos}}$  and its approximation,  $\hat{\Gamma}_{\text{pos}} = \Gamma_{\text{pr}} - KK^\top$ , as a function of the rank of  $KK^\top$  for 100 different realizations of  $H$  and  $\Gamma_{\text{pr}}$ . The third row shows, for each realization of  $(H, \Gamma_{\text{pr}})$  and for each fixed rank of  $KK^\top$ , the difference between the Förstner distance obtained with a prior- or Hessian-based dimensionality reduction technique and the minimum distance obtained with the generalized approximation. All of these differences are positive—a confirmation of Theorem 2.3. But Figure 5.1 also shows interesting patterns consistent with the observations made for the simple example above. When the spectrum of  $H$  is basically flat (left column), the directions along which the prior variance is most reduced are likely to be those corresponding to the largest prior variances, and thus a prior-based reduction is almost as

effective as the generalized one (as seen in the bottom two rows on the left). As we move to the third column, eigenvalues of  $H^{-1}$  increase more quickly. The data provide significant information only on a lower-dimensional subspace of the parameter space. In this case, it is crucial to combine this information with the directions in the parameter space along which the prior variance is the greatest. The generalized reduction technique successfully accomplishes this task, whereas the prior and Hessian reductions fail as they focus either on  $\Gamma_{\text{pr}}$  or  $H$  alone; the key is to combine the two.

In Figure 5.2 the situation is reversed and the results are symmetric to those of Figure 5.1. The spectrum of  $H$  (red) is now kept fixed with parameters  $\lambda_0 = 500$ ,  $\alpha = 1$ , and  $\tau = 10^{-9}$ , while the spectrum of  $\Gamma_{\text{pr}}$  (blue) has parameters  $\tilde{\lambda}_0 = 1$  and  $\tilde{\tau} = 10^{-9}$  with decay rates increasing from left to right:  $\tilde{\alpha} = 0.552$  (left),  $\tilde{\alpha} = 1.103$  (middle), and  $\tilde{\alpha} = 2.759$  (right). In the first column, the spectrum of the prior is nearly flat. That is, the prior variance is almost equally spread along every direction in the parameter space. In this case, the eigenstructure of  $H$  determines the directions of greatest variance reduction, and the Hessian-based reduction is almost as effective as the generalized one. As we move towards the third column, the spectrum of  $\Gamma_{\text{pr}}$  decays more quickly. The prior variance is restricted to lower-dimensional subspaces of the parameter space. Mismatch between prior- and Hessian-dominated directions then leads to poor performance of both the prior- and Hessian-based reduction techniques. However, generalized reduction performs well also in this more challenging case.

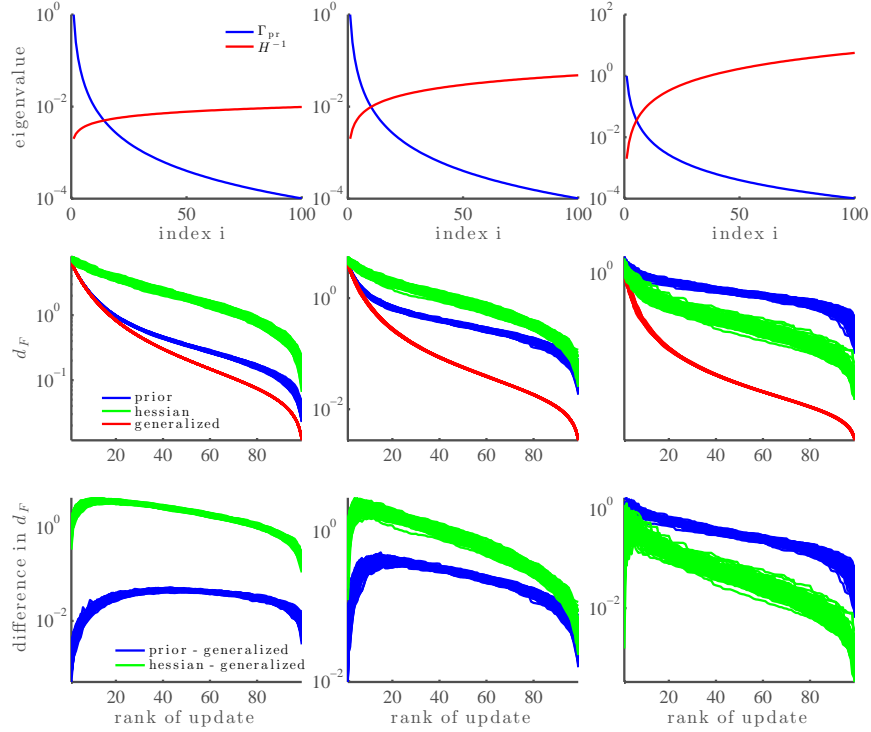


FIG. 5.1. Top row: Eigenspectra of  $\Gamma_{\text{pr}}$  (blue) and  $H^{-1}$  (red) for three values for the decay rate of the eigenvalues of  $H$ :  $\alpha = 0.345$  (left),  $\alpha = 0.690$  (middle) and  $\alpha = 1.724$  (right). Second row: Forstner distance between  $\Gamma_{\text{pos}}$  and its approximation versus the rank of the update for 100 realizations of  $\Gamma_{\text{pr}}$  and  $H$  using prior-based (blue), Hessian-based (green), and optimal (red) updates. Bottom row: Differences of posterior covariance approximation error (measured with the Forstner metric) between the prior-based and optimal updates (blue) and between the Hessian-based and optimal updates (green).

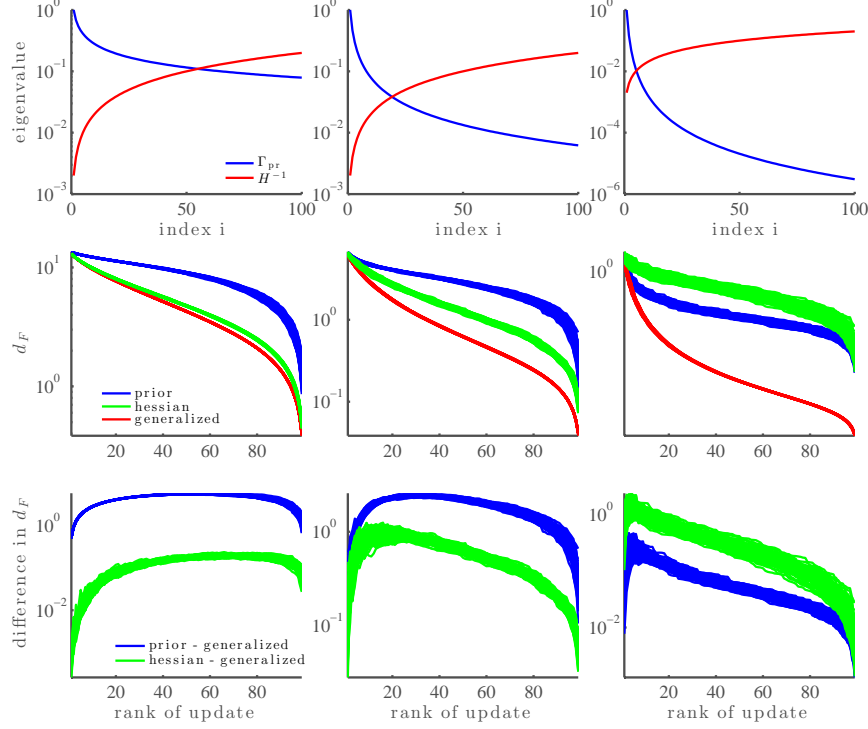


FIG. 5.2. Analogous to Figure 5.1 but this time the spectrum of  $H$  is fixed, while that of  $\Gamma_{pr}$  has varying decay rates:  $\tilde{\alpha} = 0.552$  (left),  $\tilde{\alpha} = 1.103$  (middle) and  $\tilde{\alpha} = 2.759$  (right).

**5.2. Example 2: X-ray tomography.** We consider a classical inverse problem of X-ray computed tomography (CT), where X-rays travel from sources to detectors through an object of interest. The intensities from multiple sources are measured at the detectors, the goal is to reconstruct the density of the object. In this framework, we investigate the performance of the optimal mean and covariance matrix approximations presented in Sections 2 and 4.

We model the absorption of an X-ray along a line  $\ell_i$  using Beer's law:

$$I_d = I_s \exp \left( - \int_{\ell_i} x(s) ds \right), \quad (5.1)$$

where  $I_d$  and  $I_s$  are the intensities at the detector and at the source, respectively, and  $x(s)$  is the density of the object at position  $s$  on the line  $\ell_i$ . The computational domain is discretized into a grid and the density is assumed to be constant within each grid cell. The line integrals are approximated as

$$\int_{\ell_i} x(s) ds \approx \sum_{j=1}^{\# \text{ of cells}} a_{ij} x_j, \quad (5.2)$$

where  $a_{ij}$  is the length of the intersection between line  $\ell_i$  and cell  $j$ , and  $x_j$  is the unknown density in cell  $j$ . The vector of absorptions along  $m$  lines can then be approximated as

$$I_d \approx I_s \exp(-Ax), \quad (5.3)$$

where  $I_d$  is the vector of  $m$  intensities at the detectors and  $A$  is the  $m \times n$  matrix of intersection lengths for each of the  $m$  lines. Even though the forward operator (5.3) is nonlinear, the inference

problem can be recast in a linear fashion by taking logarithm of both sides of (5.3). This leads to the following linear model for the inversion:  $y = Ax + \epsilon$ , where the measurement vector is  $y = -\log(I_d/I_s)$  and the measurement errors are assumed to be iid Gaussian,  $\epsilon \sim \mathcal{N}(0, \sigma^2 I)$ .

The setup for the inference problem, borrowed from [17], is as follows. The rectangular domain is discretized with an  $n \times n$  grid. The true object consists of three circular inclusions, each of uniform density, inside an annulus. Ten X-ray sources are positioned on one side of a circle, and each source sends a fan of 100 X-rays that are measured by detectors on the opposite side of the object. Here, the 10 sources are distributed evenly so that they form a total illumination angle of 90 degrees, resulting in a limited-angle CT problem. We use the exponential model (5.1) to generate synthetic data in a discretization-independent fashion by computing the exact intersections between the rays and the circular inclusions in the domain. Gaussian noise with standard deviation  $\sigma = 0.002$  is added to the simulated data. The imaging setup and data from one source are illustrated in Figure 5.3.

The unknown density is estimated on a  $128 \times 128$  grid. Thus the discretized vector  $x$  has length 16384, and direct computation of the posterior mean and the posterior covariance matrix, as well as generation of posterior samples, can be computationally nontrivial. To define the prior distribution,  $x$  is modeled as a discretized solution of a stochastic PDE of the form:

$$\gamma (\kappa^2 \mathcal{I} - \Delta) x(s) = \mathcal{W}(s), \quad s \in \Omega, \quad (5.4)$$

where  $\mathcal{W}$  is a white noise process,  $\Delta$  is the Laplacian operator, and  $\mathcal{I}$  is the identity operator. The solution of (5.4) is a Gaussian random field whose correlation length and variance are controlled by the free parameters  $\kappa$  and  $\gamma$ , respectively. A square root of the prior precision matrix of  $x$  (which is positive definite) can then be easily computed (see [25] for details). We use  $\kappa = 10$  and  $\gamma = \sqrt{800}$  in our simulations.

Our first task is to compute an optimal approximation of  $\Gamma_{\text{pos}}$  as a low-rank negative update of  $\Gamma_{\text{pr}}$  (cf. Theorem 2.3). Figure 5.4 (top row) shows the convergence of the approximate posterior variance as the rank of the update increases. The zero-rank update corresponds to  $\Gamma_{\text{pr}}$  (first column). For this formally 16384-dimensional problem, a good approximation of the posterior variance is achieved with a rank 200 update; hence the data are informative only on a low-dimensional subspace. The quality of the covariance matrix approximation is also reflected in the structure of samples drawn from the approximate posterior distributions (bottom row). All five of these samples are drawn using the same random seed and the exact posterior mean, so that all the differences observed are due to the approximation of  $\Gamma_{\text{pos}}$ . Already with a rank 100 update, the small-scale features of the approximate posterior sample match those of the exact posterior sample. In applications, agreement in this “eye-ball norm” is important. Of course, an exact formula for the error in the posterior covariance matrix approximation is given in Theorem 2.3; it is a function only of the eigenvalues of the prior-preconditioned Hessian  $\hat{H}$ .

Our second task is to assess the performances of the two optimal posterior mean approximations given in Section 4. We will use  $\mu_{\text{pos}}^{(r)}(y)$  to denote the low-rank approximation and  $\hat{\mu}_{\text{pos}}^{(r)}(y)$  to denote the low-rank *update* approximation. Recall that both approximations are linear functions of the data  $y$ , given by  $\mu_{\text{pos}}^{(r)}(y) = A^* y$  with  $A^* \in \mathcal{A}_r$  and  $\hat{\mu}_{\text{pos}}^{(r)}(y) = \hat{A}^* y$  with  $\hat{A}^* \in \hat{\mathcal{A}}_r$ , where the classes  $\mathcal{A}_r$  and  $\hat{\mathcal{A}}_r$  are defined in (4.2). As in Section 4, we shall use  $\mathcal{A}$  to denote either of the two classes.

Figure 5.5 shows the normalized error  $\|\mu(y) - \mu_{\text{pos}}(y)\|_{\Gamma_{\text{pos}}^{-1}} / \|\mu_{\text{pos}}(y)\|_{\Gamma_{\text{pos}}^{-1}}$  for different approximations  $\mu(y)$  of the true posterior mean  $\mu_{\text{pos}}(y)$  and a fixed realization  $y$  of the data. The error is a function of the order  $r$  of the approximation class  $\mathcal{A}$ . Snapshots of  $\mu(y)$  are shown along the two error curves. For reference,  $\mu_{\text{pos}}(y)$  is also shown at the top. We see that the errors decrease monotonically, but that the low-rank approximation outperforms the low-rank update approximation for lower values of  $r$ . This is consistent with the discussion at the end of Section 4; the crossing point of the error curves is also consistent with that analysis. In particular, we expect the low-rank update approximation to outperform the low-rank approximation only when the approximation starts to



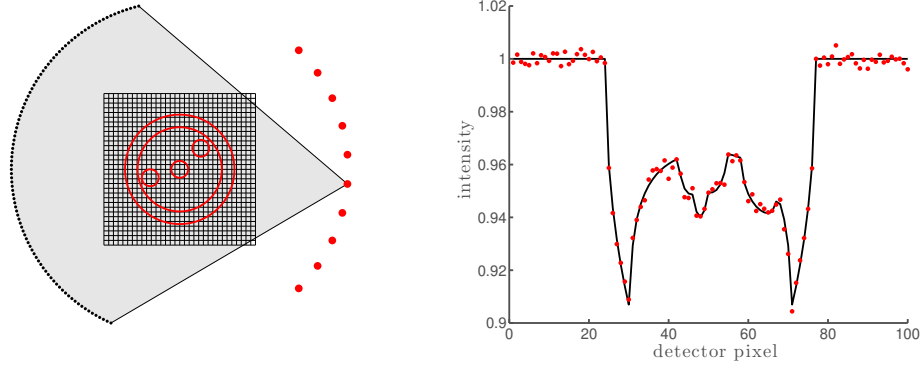


FIG. 5.3. *X-ray tomography problem. Left: Discretized domain, true object, sources (red dots), and detectors corresponding to one source (black dots). The fan transmitted by one source is illustrated in gray. The density of the object is 0.006 in the outer ring and 0.004 in the three inclusions; the background density is zero. Right: The true simulated intensity (black line) and noisy measurements (red dots) for one source.*

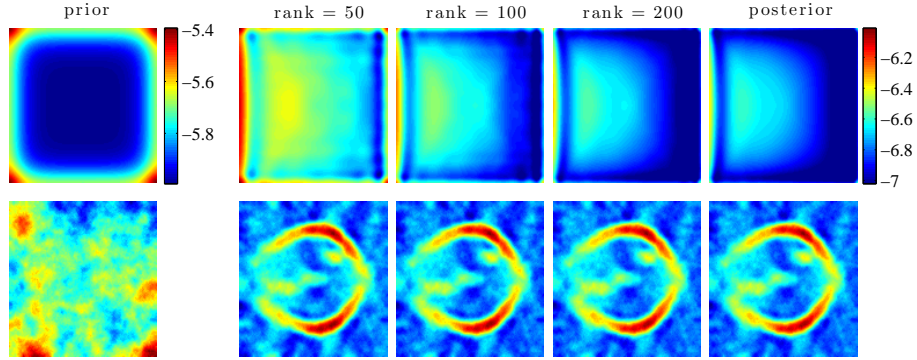


FIG. 5.4. *X-ray tomography problem. First column: Prior variance field, in log scale (top), and a sample drawn from the prior distribution (bottom). Second through last columns (left to right): Variance field, in log scale, of the approximate posterior as the rank of the update increases (top); samples from the corresponding approximate posterior distributions (bottom) assuming exact knowledge of the posterior mean.*

include generalized eigenvalues of the pencil  $(H, \Gamma_{\text{pr}}^{-1})$  that are less than one—i.e., once the approximations are no longer *under-resolved*. This can be confirmed by comparing Figure 5.5 with the decay of the generalized eigenvalues of the pencil  $(H, \Gamma_{\text{pr}}^{-1})$  in the right panel of Figure 5.7 (blue curve).

On top of each snapshot in Figure 5.5, we show the *relative CPU time* required to compute the corresponding posterior mean approximation. The relative CPU time is defined as the time required to compute this approximation divided by the time required to apply the posterior precision matrix to a vector. The latter is the essential element of computing the posterior mean via an iterative solver, such as a Krylov subspace method, and these solvers are the standard choice for computing the posterior mean in large-scale inverse problems. Evaluating the ratio allows us to determine how many solver iterations we could perform with a computational cost roughly equal to that of our approximations. Based on the reported times, a few observations can be made. First of all, as anticipated in Section 4, computing  $\mu_{\text{pos}}^{(r)}(y)$  for any new realization of the data is faster than computing  $\hat{\mu}_{\text{pos}}^{(r)}(y)$ . Second, obtaining an accurate posterior mean approximation requires roughly  $r = 200$ , and the relative CPU times for this order of approximation are 7.3 for  $\mu_{\text{pos}}^{(r)}(y)$  and 29.0

for  $\hat{\mu}_{\text{pos}}^{(r)}(y)$ ; these are roughly the number of iterations of an iterative solver that one could take for equivalent computational cost. That is, the speedup of the posterior mean approximation compared to an iterative solver is not particularly dramatic in this case, because the forward model  $A$  is simply a sparse matrix that is cheap to apply. For the heat equation example discussed in Section 5.3, the situation is different.

Note that the above computational time estimates exclude other costs associated with iterative solvers. For instance, preconditioners are often applied; these significantly decrease the number of iterations needed for the solvers to converge but, on the other hand, increase the cost per iteration. A popular approach for solving the posterior mean efficiently is to use the prior covariance as the preconditioner [2]. In the limited-angle tomography problem, including the application of this preconditioner in the reference CPU time would reduce the relative CPU time of our  $r = 200$  approximations to 0.48 for  $\mu_{\text{pos}}^{(r)}(y)$  and 1.9 for  $\hat{\mu}_{\text{pos}}^{(r)}(y)$ . That is, the cost of computing our approximations is roughly equal to *one iteration* of a prior-preconditioned iterative solver. The large difference compared to the case without preconditioning is due to the fact that applying the prior here is computationally much heavier than applying the forward model.

Figure 5.6 (left panel) shows unnormalized errors in the approximation of  $\mu_{\text{pos}}(y)$ ,

$$\|e(y)\|_{\Gamma_{\text{pos}}^{-1}}^2 = \|\mu_{\text{pos}}^{(r)}(y) - \mu_{\text{pos}}(y)\|_{\Gamma_{\text{pos}}^{-1}}^2 \quad \text{and} \quad \|\hat{e}(y)\|_{\Gamma_{\text{pos}}^{-1}}^2 = \|\hat{\mu}_{\text{pos}}^{(r)}(y) - \mu_{\text{pos}}(y)\|_{\Gamma_{\text{pos}}^{-1}}^2, \quad (5.5)$$

for the same realization of  $y$  used in Figure 5.5. In the same panel, we also show the expected values of these errors over the prior predictive distribution of  $y$ , which is exactly the  $r$ -dependent component of the Bayes risk given in Theorems 4.1 and 4.2. Both sets of errors decay with increasing  $r$  and show a similar crossover between the two approximation classes. But the particular error  $\|e(y)\|_{\Gamma_{\text{pos}}^{-1}}^2$  departs consistently from its expectation; this is not unreasonable in general (the mean estimator has a nonzero variance), but the offset may be accentuated in this case because the data are generated from an image that is not drawn from the prior. (The right panel of Figure 5.6, which comes from Example 3, represents a contrasting case.)

By design, the posterior approximations described in this paper perform well when the data inform a low-dimensional subspace of the parameter space. To better understand this effect, we also consider a *full-angle* configuration of the tomography problem, wherein the sources and detectors are evenly spread around the entire unknown object. In this case, the data are more informative than in the limited-angle configuration. This can be seen in the decay rate of the generalized eigenvalues of the pencil  $(H, \Gamma_{\text{pr}}^{-1})$  in the right panel of Figure 5.7 (blue and red curves); eigenvalues for the full-angle configuration decay more slowly than for the limited-angle configuration. Thus, according to the optimal loss given in (2.10) (Theorem 2.3), the prior-to-posterior update in the full-angle case must be of greater rank than the update in the limited-angle case for any given approximation error. Also, good approximation of  $\mu_{\text{pos}}(y)$  in the full-angle case requires higher order of the approximation class  $\mathcal{A}$ , as is shown in Figure 5.8. But because the data are strongly informative, they allow an almost perfect reconstruction of the underlying truth image. The relative CPU times are similar to the limited angle case: roughly 8 for  $\mu_{\text{pos}}^{(r)}(y)$  and 14 for  $\hat{\mu}_{\text{pos}}^{(r)}(y)$ . If preconditioning with the prior covariance is included in the reference CPU time calculation, the relative CPU times drop to 1.5 for  $\mu_{\text{pos}}^{(r)}(y)$  and to 2.6 for  $\hat{\mu}_{\text{pos}}^{(r)}(y)$ .

**5.3. Example 3: Heat equation.** Our last example is the classic linear inverse problem of solving for the initial conditions of an inhomogeneous heat equation. Let  $u(s, t)$  be the time dependent state of the heat equation on  $s = (s_1, s_2) \in \Omega = [0, 1]^2$ ,  $t \geq 0$ , and let  $\kappa(s)$  be the heat conductivity field. Given initial conditions  $u_0(s) = u(s, 0)$ , the state evolves in time according to the linear heat equation:

$$\begin{aligned} \frac{\partial u(s, t)}{\partial t} &= -\nabla \cdot (\kappa(s) \nabla u(s, t)), & s \in \Omega, \quad t > 0, \\ \kappa(s) \nabla u(s, t) \cdot n(s) &= 0, & s \in \partial\Omega, \quad t > 0, \end{aligned} \quad (5.6)$$

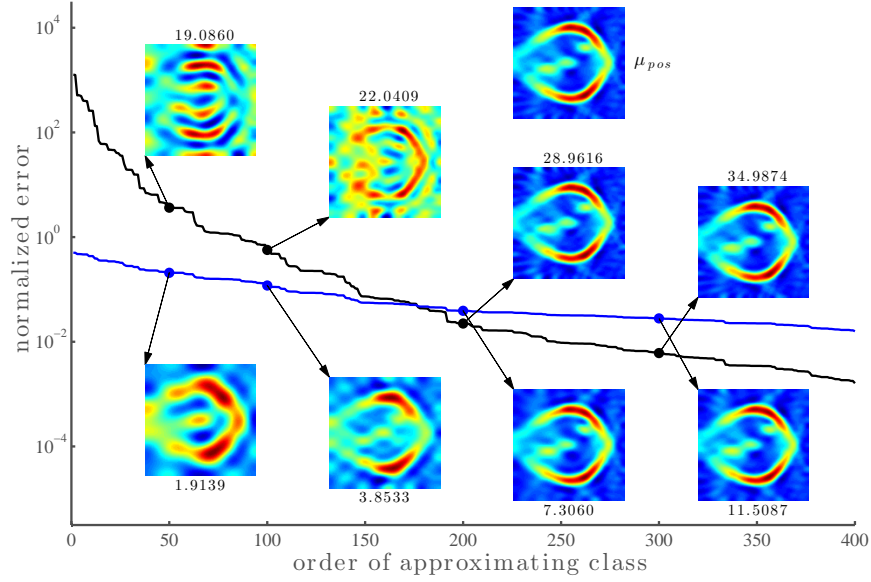


FIG. 5.5. *Limited-angle X-ray tomography: Comparison of the optimal posterior mean approximations,  $\mu_{\text{pos}}^{(r)}(y)$  (blue) and  $\hat{\mu}_{\text{pos}}^{(r)}(y)$  (black) of  $\mu_{\text{pos}}(y)$  for a fixed realization of the data  $y$ , as a function of the order  $r$  of the approximating classes  $\mathcal{A}_r$  and  $\hat{\mathcal{A}}_r$ , respectively. The normalized error for an approximation  $\mu(y)$  is defined as  $\|\mu(y) - \mu_{\text{pos}}(y)\|_{\Gamma_{\text{pos}}^{-1}} / \|\mu_{\text{pos}}(y)\|_{\Gamma_{\text{pos}}^{-1}}$ . The numbers above or below the snapshots indicate the relative CPU time of the corresponding mean approximation—i.e., the time required to compute the approximation divided by the time required to apply the posterior precision matrix to a vector.*

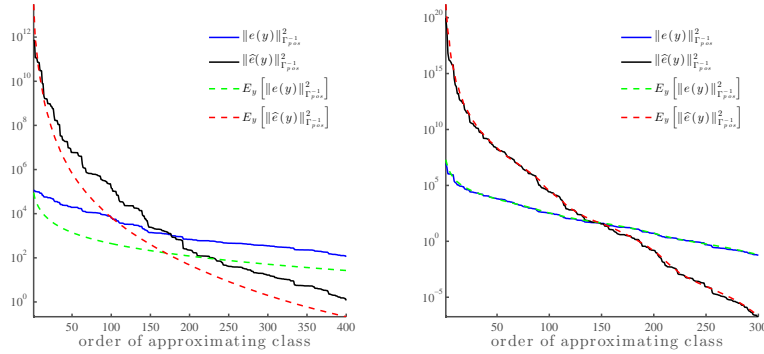


FIG. 5.6. *The errors  $\|e(y)\|_{\Gamma_{\text{pos}}^{-1}}^2$  (blue) and  $\|\hat{e}(y)\|_{\Gamma_{\text{pos}}^{-1}}^2$  (black) defined by (5.5), and their expected values in green and red, respectively; for Example 2 (left panel) and Example 3 (right panel).*

where  $n(s)$  denotes the outward-pointing unit normal at  $s \in \partial\Omega$ . We place  $n_s = 81$  sensors at the locations  $s_1, \dots, s_{n_s}$ , uniformly spaced within the lower left quadrant of the spatial domain, as illustrated by the black dots in Figure 5.9. We use a finite dimensional discretization of the parameter space based on the finite element method on a regular  $100 \times 100$  grid,  $\{s'_i\}$ . Our goal is to infer the vector  $x = (u_0(s'_i))$  of initial conditions on the grid. Thus, the dimension of the parameter space for the inference problem is  $n = 10^4$ . We use data measured at 50 discrete times  $t = t_1, t_2, \dots, t_{50}$ , where  $t_i = i\Delta t$ , and  $\Delta t = 2 \times 10^{-4}$ . At each time  $t_i$ , pointwise observations of

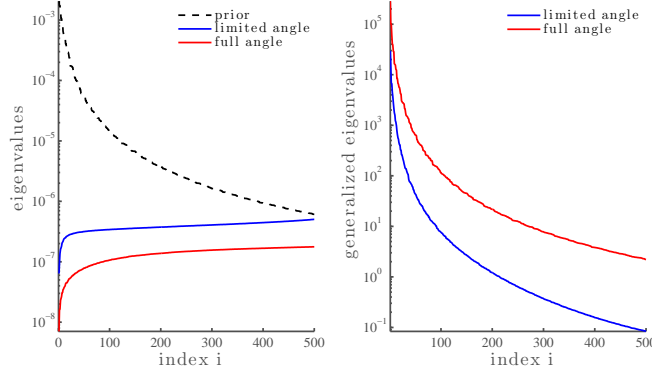


FIG. 5.7. Left: Leading eigenvalues of  $\Gamma_{\text{pr}}$  and  $H^{-1}$  in the limited-angle and full-angle X-ray tomography problems. Right: Leading generalized eigenvalues of the pencil  $(H, \Gamma_{\text{pr}}^{-1})$  in the limited-angle (blue) and full-angle (red) cases.

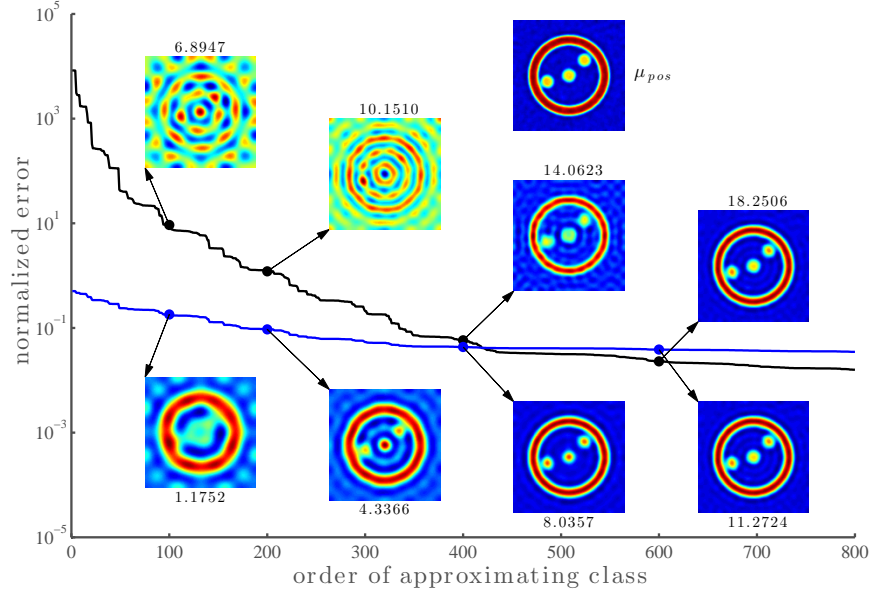


FIG. 5.8. Same as Figure 5.5, but for full-angle X-ray tomography (sources and receivers spread uniformly around the entire object).

the state  $u$  are taken at these sensors, i.e.,

$$d_i = \mathcal{C}u(s, t_i), \quad (5.7)$$

where  $\mathcal{C}$  is the observation operator that maps the function  $u(s, t_i)$  to  $d = (u(s_1, t_i), \dots, u(s_n, t_i))^T$ . The vector of observations is then  $d = [d_1; d_2; \dots; d_{50}]$ . The noisy data vector is  $y = d + \varepsilon$ , where  $\varepsilon \sim \mathcal{N}(0, \sigma^2 I)$  and  $\sigma = 10^{-2}$ . Note that the data are a linear function of the initial conditions, perturbed by Gaussian noise. Thus the data can be written as:

$$y = Ax + \varepsilon, \quad \varepsilon \sim \mathcal{N}(0, \sigma^2 I). \quad (5.8)$$

where  $A$  is a linear map defined by the composition of the forward model (5.6) with the observation operator (5.7), both linear.

We generate synthetic data by evolving the initial conditions shown in Figure 5.9. This “true” value of the inversion parameters  $x$  is a discretized realization of a Gaussian process satisfying an SPDE of the same form used in the previous tomography example, but now with a non-stationary permeability field. In other words, the truth is a draw from the prior in this example (unlike in the previous example), and the prior Gaussian process satisfies the following SPDE:

$$\gamma (\kappa^2 \mathcal{I} - \nabla \cdot \mathbf{c}(s) \nabla) x(s) = \mathcal{W}(s) \quad s \in \Omega, \quad (5.9)$$

where  $\mathbf{c}(s)$  is the space-dependent permeability tensor. One can visualize the resulting prior variance field in Figure 5.10 (first column, top row).

Figures 5.10 and 5.11, along with the right panel in Figure 5.5, show our numerical results. They have the same interpretation as Figures 5.4–5.6 in the tomography example. The trends in the figures are consistent with those encountered in the previous example and confirm the good performance of the optimal low-rank approximation. In Figure 5.10 we see that the lowest posterior variance regions correspond to the positions of the sensors. Since the sensors are sparse and localized, one would expect the data to be informative only on a low-dimensional subspace of the parameter space. This is confirmed by the low order of the approximation needed to accurately capture the posterior variance field and the posterior mean (Figures 5.10 and 5.11). Notice that in Figures 5.11 and 5.5, the approximation of the posterior mean appears to be nearly perfect (visually) once the error curves for the two approximations cross. This is somewhat expected from the theory since we know that the crossing point should occur when the approximations start to use eigenvalues of the prior-preconditioned Hessian that are less than one—that is, once we have exhausted directions in the parameter space where the data are more constraining than the prior.

Again, we report the relative CPU time for each posterior mean approximation above/below the corresponding snapshot in Figure 5.11. The results differ significantly from the tomography example. For instance, at order  $r = 200$ , which yields approximations that are visually indistinguishable from the true mean, the relative CPU times are 0.001 for  $\mu_{\text{pos}}^{(r)}(y)$  and 0.53 for  $\hat{\mu}_{\text{pos}}^{(r)}(y)$ . Therefore we can compute an accurate mean approximation much more quickly than taking one iteration of an iterative solver. The difference between this case and tomography example of Section 5.2 is due to the higher CPU cost of applying the forward and adjoint models for the heat equation—solving a PDE versus applying a sparse matrix. Also, because the cost of applying the prior covariance is negligible compared to that of the forward and adjoint solves in this example, preconditioning the iterative solver with the prior would not strongly affect the reported relative CPU times, unlike the tomography example.

Figure 5.12 illustrates some important directions characterizing the heat equation inverse problem. The first two columns show the four leading eigenvectors of, respectively,  $\Gamma_{\text{pr}}$  and  $H$ . Notice that the support of the eigenvectors of  $H$  concentrates around the sensors. The third column shows the four leading directions ( $\hat{w}_i$ ) defined in Theorem 2.3. These directions define the optimal prior-to-posterior covariance matrix update (cf. (2.9)). This update of  $\Gamma_{\text{pr}}$  is *necessary* to capture directions ( $\tilde{w}_i$ ) of greatest relative difference between prior and posterior variance (cf. Corollary 3.1). The four leading directions ( $\tilde{w}_i$ ) are shown in the fourth column. The support of these modes is again concentrated around the sensors, which intuitively makes sense as these are directions of greatest variance reduction.

**6. Conclusions.** This paper has presented and characterized optimal approximations of the Bayesian solution of linear inverse problems, with Gaussian prior and noise distributions defined on finite-dimensional spaces. In a typical large-scale inverse problem, observations may be informative—relative to the prior—only on a low-dimensional subspace of the parameter space. Our approximations therefore identify and exploit low-dimensional structure in the *update* from prior to posterior.

We have developed two types of optimality results. In the first, the posterior covariance matrix is approximated as a low-rank negative semidefinite update of the prior covariance matrix. We

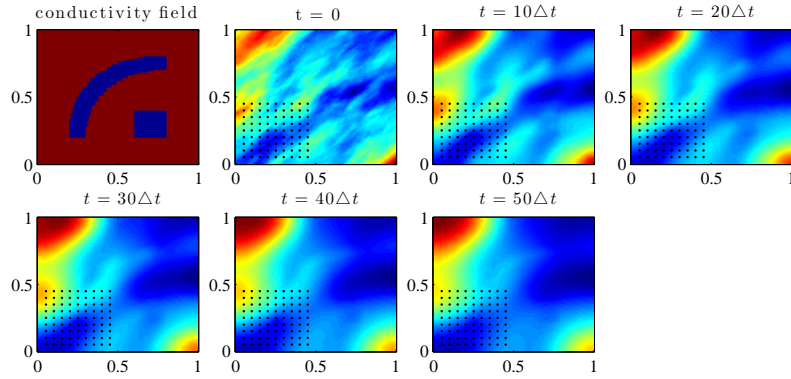


FIG. 5.9. Heat equation (Example 3). Initial condition (top left) and several snapshots of the states at different times. Black dots indicate sensor locations.

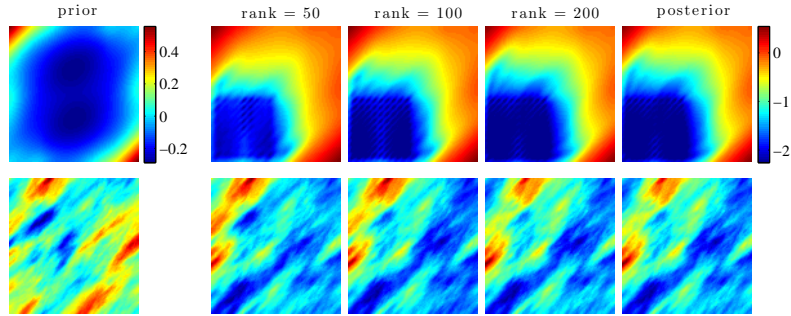


FIG. 5.10. Same as Figure 5.4, but for Example 3 (initial condition inversion for the heat equation).

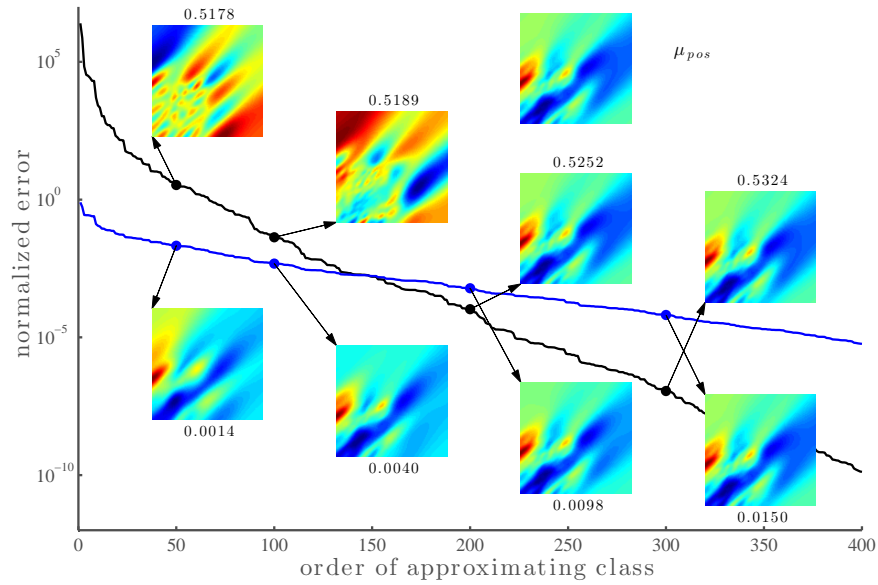


FIG. 5.11. Same as Figure 5.5, but for Example 3 (initial condition inversion for the heat equation).



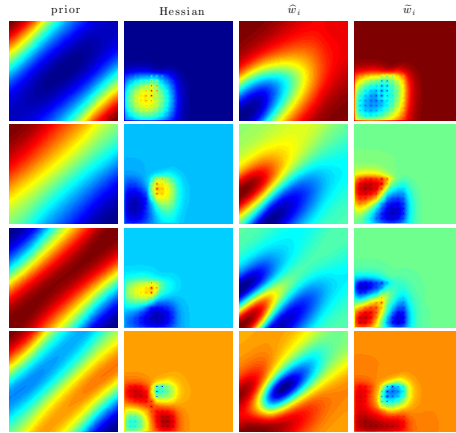


FIG. 5.12. *Heat equation (Example 3). First column: Four leading eigenvectors of  $\Gamma_{\text{pr}}$ . Second column: Four leading eigenvectors of  $H$ . Third column: Four leading directions ( $\hat{w}_i$ ) (cf. (2.9)). Fourth column: Four leading directions ( $\tilde{w}_i$ ) (cf. Corollary 3.1)*

describe an update of this form that is optimal with respect to a broad class of loss functions between covariance matrices, exemplified by the Förstner metric [13] for symmetric positive definite matrices. We argue that this is the appropriate class of loss functions with which to evaluate approximations of the posterior covariance matrix, and show that optimality in such metrics identifies directions in parameter space along which the posterior variance is reduced the most, relative to the prior. Optimal low-rank updates are derived from a generalized eigendecomposition of the pencil defined by the log-likelihood Hessian and the prior precision matrix. These updates have been proposed in previous work [12], but our work complements these efforts by characterizing the optimality of the resulting approximations. Under the assumption of exact knowledge of the posterior mean, our results extend to optimality statements between the associated distributions (e.g., optimality in the Hellinger distance and in the Kullback-Leibler divergence). Second, we have developed fast approximations of the posterior mean that are useful when repeated evaluations thereof are required for multiple realizations of the data (e.g., in an online inference setting). These approximations are optimal in the sense that they minimize the Bayes risk for squared-error loss induced by the posterior precision matrix. The most computationally efficient of these approximations expresses the posterior mean as the product of a single low-rank matrix with the data. We have demonstrated the covariance and mean approximations numerically on a variety of inverse problems: synthetic problems constructed from random Hessian and prior covariance matrices; an X-ray tomography problem with different observation scenarios; and inversion for the initial condition of a heat equation, with localized observations and a non-stationary prior.

This work has several extensions, some of which are already part of ongoing research. First, it is natural to generalize the present approach to infinite-dimensional parameter spaces endowed with Gaussian priors. This setting is essential to understanding and formalizing Bayesian inference over function spaces [5, 31]. Here, by analogy with the current results, one would expect the posterior covariance operator to be well approximated by a finite-rank negative perturbation of the prior covariance operator. A further extension could allow the data to become infinite-dimensional as well. Another important task is to generalize the present methodology to inverse problems with nonlinear forward models. One approach for doing so is presented in [11]; other approaches are certainly possible. Yet another interesting research topic is the study of analogous approximation techniques for sequential inference. We note that the assimilation step in a linear (or linearized) data assimilation scheme can be already tackled within the framework presented here. But the nonstationary setting, where inference is interleaved with evolution of the state, introduces the



possibility for even more tailored and structure-exploiting approximations.

**Acknowledgments.** This work was supported by the US Department of Energy, Office of Advanced Scientific Computing (ASCR), under grant numbers DE-SC0003908 and DE-SC0009297. We thank J. Heikkinen from Bintec Ltd. for providing us with the code used in Example 2.

**Appendix A. Technical results.** Here we collect the proofs and other technical results necessary to support the statements made in the previous sections.

We start with an auxiliary approximation result that plays an important role in our analysis. Given a semi-positive definite diagonal matrix  $D$ , we seek an approximation of  $D + I$  by a rank  $r$  perturbation of the identity,  $UU^\top + I$ , that minimizes a loss function from the class  $\mathcal{L}$  defined in (2.6). The following lemma shows that the optimal solution  $\hat{U}\hat{U}^\top$  is simply the best rank  $r$  approximation of the matrix  $D$  in the Frobenius norm.

**LEMMA A.1** (Approximation lemma). *Let  $D = \text{diag}\{d_1^2, \dots, d_n^2\}$ , with  $d_i^2 \geq d_{i+1}^2$ , and  $L \in \mathcal{L}$ . Define the functional  $\mathcal{J} : \mathbb{R}^{n \times r} \rightarrow \mathbb{R}$ , as:  $\mathcal{J}(U) = L(UU^\top + I, D + I) = \sum_i f(\sigma_i)$ , where  $(\sigma_i)$  are the generalized eigenvalues of the pencil  $(UU^\top + I, D + I)$  and  $f \in \mathcal{U}$ . Then:*

(i) *There is a minimizer,  $\hat{U}$ , of  $\mathcal{J}$  such that*

$$\hat{U}\hat{U}^\top = \sum_{i=1}^r d_i^2 e_i e_i^\top. \quad (\text{A.1})$$

*where  $(e_i)$  are the columns of the identity matrix.*

(ii) *If the first  $r$  eigenvalues of  $D$  are distinct, then any minimizer of  $\mathcal{J}$  satisfies (A.1).*

*Proof.* The idea is to apply [21, Theorem 1.1] to the functional  $\mathcal{J}$ . To this end, we notice that  $\mathcal{J}$  can be equivalently written as:  $\mathcal{J}(U) = F \circ \rho_n \circ g(U)$ , where:  $F : \mathbb{R}_+^n \rightarrow \mathbb{R}$  is of the form  $F(x) = \sum_{i=1}^n f(x_i)$ ;  $\rho_n$  denotes a function that maps an  $n \times n$  SPD matrix  $A$  to its eigenvalues  $\sigma = (\sigma_i)$  (i.e.,  $\rho_n(A) = \sigma$  and since  $F$  is a symmetric function, the order of the eigenvalues is irrelevant); and the mapping  $g$  is given by:  $g(U) = (D + I)^{-1/2}(UU^\top + I)(D + I)^{-1/2}$ , for all  $U \in \mathbb{R}^{n \times r}$ . Since the function  $F \circ \rho_n$  satisfies the hypotheses in [21, Theorem 1.1],  $F \circ \rho_n$  is differentiable at the SPD matrix  $X$  if and only if  $F$  is differentiable at  $\rho_n(X)$ , in which case  $(F \circ \rho_n)'(X) = ZS_\sigma Z^\top$ , where

$$S_\sigma = \text{diag}[F'(\rho_n(X))] = \text{diag}\{f'(\sigma_1), \dots, f'(\sigma_n)\},$$

and  $Z$  is an orthogonal matrix such that  $X = Z \text{diag}[\rho_n(X)]Z^\top$ . Using the chain rule, we obtain

$$\frac{\partial \mathcal{J}(U)}{\partial U_{ij}} = \text{tr} \left( ZS_\sigma Z^\top \frac{\partial g(U)}{\partial U_{ij}} \right),$$

which leads to the following gradient of  $\mathcal{J}$  at  $U$ :

$$\mathcal{J}'(U) = 2(D + I)^{-1/2} ZS_\sigma (D + I)^{-1/2} Z^\top U = 2WS_\sigma W^\top U,$$

where the orthogonal matrix  $Z$  is such that the matrix  $W = (D + I)^{-1/2}Z$  satisfies

$$(UU^\top + I)W = (D + I)W\Upsilon_\sigma \quad (\text{A.2})$$

with  $\Upsilon_\sigma = \text{diag}(\sigma)$ . Now we show that the functional  $\mathcal{J}$  is coercive. Let  $(U_k)$  be a sequence of matrices such that  $\|U_k\|_F \rightarrow \infty$ . Hence,  $\sigma_{\max}(g(U_k)) \rightarrow \infty$  and so does  $\mathcal{J}$  since:

$$\mathcal{J}(U_k) \geq f(\sigma_{\max}(g(U_k))) + (n - 1)f(1)$$

and  $f(x) \rightarrow \infty$  as  $x \rightarrow \infty$ . Thus,  $\mathcal{J}$  is a differentiable coercive functional, and has a global minimizer  $\hat{U}$  with zero gradient:

$$\mathcal{J}'(\hat{U}) = 2WS_\sigma W^\top \hat{U} = 0. \quad (\text{A.3})$$

However, since  $f \in \mathcal{U}$ ,  $f'(x) = 0$  iff  $x = 1$ . It follows that condition (A.3) is equivalent to

$$(I - \Upsilon_\sigma)W^\top \widehat{U} = 0. \quad (\text{A.4})$$

(A.2) and (A.4) give  $\widehat{U}\widehat{U}^\top - D = W^{-\top}\Upsilon^{-1}(\Upsilon - I)W^\top$ , and right-multiplication by  $\widehat{U}\widehat{U}^\top$  then yields:

$$D(\widehat{U}\widehat{U}^\top) = (\widehat{U}\widehat{U}^\top)^2. \quad (\text{A.5})$$

In particular, if  $u$  is an eigenvector of  $\widehat{U}\widehat{U}^\top$  with nonzero eigenvalue  $\alpha$ , then  $u$  is an eigenvector of  $D$ ,  $Du = \alpha u$ , and thus  $\alpha = d_i^2 > 0$  for some  $i$ . Thus, any solution of (A.5) is such that:

$$\widehat{U}\widehat{U}^\top = \sum_{i=1}^{r_k} d_{k_i}^2 e_{k_i} e_{k_i}^\top, \quad (\text{A.6})$$

for some subsequence  $(k_\ell)$  of  $\{1, \dots, n\}$  and rank  $r_k \leq r$ . Notice that any  $\widehat{U}$  satisfying (A.5) is also a critical point according to (A.4). From (A.6) we also find that  $g(\widehat{U})$  is a diagonal matrix,

$$g(\widehat{U}) = (D + I)^{-1} \left( \sum_{i=1}^{r_k} d_{k_i}^2 e_{k_i} e_{k_i}^\top + I \right).$$

The diagonal entries  $\sigma_i$ , which are the eigenvalues of  $g(\widehat{U})$ , are given by  $\sigma_i = 1$  if  $i = k_\ell$  for some  $\ell \leq r_k$ , or  $\sigma_i = 1/(1 + d_i^2)$  otherwise. In either case, we have  $0 < \sigma_i \leq 1$  and the monotonicity of  $f$  implies that  $\mathcal{J}(\widehat{U})$  is minimized by the subsequence  $k_1 = 1, \dots, k_r = r$ , and by the choice  $r_k = r$ . This proves (A.1). It is clear that if the first  $r$  eigenvalues of  $D$  are distinct, then any minimizer of  $\mathcal{J}$  satisfies (A.1).  $\square$

Most of the objective functions we consider have the same structure as the loss function  $\mathcal{J}$ . Hence, the importance of Lemma A.1.

The next lemma shows that searching for a negative update of  $\Gamma_{\text{pr}}$  is equivalent to looking for a positive update of the prior precision matrix. In particular, the lemma provides a bijection between the two approximation classes,  $\mathcal{M}_r$  and  $\mathcal{M}_r^{-1}$ , defined by (2.4) and (3.1). In what follows,  $S_{\text{pr}}$  is any square root of the prior covariance matrix such that  $\Gamma_{\text{pr}} = S_{\text{pr}} S_{\text{pr}}^\top$ .

**LEMMA A.2** (Prior updates). *For any negative semidefinite update of  $\Gamma_{\text{pr}}$ ,  $\widehat{\Gamma}_{\text{pos}} = \Gamma_{\text{pr}} - KK^\top$  with  $\widehat{\Gamma}_{\text{pos}} \succ 0$ , there is a matrix  $U$  (of the same rank as  $K$ ) such that  $\widehat{\Gamma}_{\text{pos}} = (\Gamma_{\text{pr}}^{-1} + UU^\top)^{-1}$ . The converse is also true.*

*Proof.* Let  $ZDZ^\top = S_{\text{pr}}^{-1}KK^\top S_{\text{pr}}^{-\top}$ ,  $D = \text{diag}\{d_i^2\}$ , be a reduced SVD of  $S_{\text{pr}}^{-1}KK^\top S_{\text{pr}}^{-\top}$ . Since  $\widehat{\Gamma}_{\text{pos}} \succ 0$  by assumption, we must have  $d_i^2 < 1$  for all  $i$ , and we may thus define  $U = S_{\text{pr}}^{-\top} ZD^{1/2}(I - D)^{-1/2}$ . By Woodbury's identity:

$$(\Gamma_{\text{pr}}^{-1} + UU^\top)^{-1} = \Gamma_{\text{pr}} - \Gamma_{\text{pr}} U (I + U^\top \Gamma_{\text{pr}}^{-1} U)^{-1} U^\top \Gamma_{\text{pr}} = \Gamma_{\text{pr}} - KK^\top = \widehat{\Gamma}_{\text{pos}}.$$

Conversely, given a matrix  $U$ , we use again Woodbury's identity to write  $\widehat{\Gamma}_{\text{pos}}$  as a negative semidefinite update of  $\Gamma_{\text{pr}}$ :  $\widehat{\Gamma}_{\text{pos}} = \Gamma_{\text{pr}} - KK^\top \succ 0$ .  $\square$

Now we prove our main result on approximations of the posterior covariance matrix.

**Proof of Theorem 2.3.** Given a loss function  $L \in \mathcal{L}$ , our goal is to minimize:

$$L(\Gamma_{\text{pos}}, \widehat{\Gamma}_{\text{pos}}) = \sum_i f(\sigma_i) \quad (\text{A.7})$$

over  $K \in \mathbb{R}^{n \times r}$  subject to the constraint  $\widehat{\Gamma}_{\text{pos}} = \Gamma_{\text{pr}} - KK^\top \succ 0$ , where  $(\sigma_i)$  are the generalized eigenvalues of the pencil  $(\Gamma_{\text{pos}}, \widehat{\Gamma}_{\text{pos}})$  and  $f$  belongs to the class  $\mathcal{U}$  defined by Eq. (2.7). We also

write  $\sigma_i(\Gamma_{\text{pos}}, \widehat{\Gamma}_{\text{pos}})$  to specify the pencil corresponding to the eigenvalues. By Lemma A.2, the optimization problem is equivalent to finding a matrix,  $U \in \mathbb{R}^{n \times r}$ , that minimizes (A.7) subject to  $\widehat{\Gamma}_{\text{pos}}^{-1} = \Gamma_{\text{pr}}^{-1} + UU^\top$ . Observe that  $(\sigma_i)$  are also the eigenvalues of the pencil  $(\widehat{\Gamma}_{\text{pos}}^{-1}, \Gamma_{\text{pos}}^{-1})$ .

Let  $WDW^\top = S_{\text{pr}}^\top H S_{\text{pr}}$  with  $D = \text{diag}\{\delta_i^2\}$ , be an SVD of  $S_{\text{pr}}^\top H S_{\text{pr}}$ . Then, by the invariance properties of the generalized eigenvalues we have:

$$\sigma_i(\widehat{\Gamma}_{\text{pos}}^{-1}, \Gamma_{\text{pos}}^{-1}) = \sigma_i(W^\top S_{\text{pr}}^\top \widehat{\Gamma}_{\text{pos}}^{-1} S_{\text{pr}} W, W^\top S_{\text{pr}}^\top \Gamma_{\text{pos}}^{-1} S_{\text{pr}} W) = \sigma_i(ZZ^\top + I, D + I),$$

where  $Z = W^\top S_{\text{pr}}^\top U$ . Therefore, our goal reduces to finding a matrix,  $Z \in \mathbb{R}^{n \times r}$ , that minimizes (A.7) with  $(\sigma_i)$  being the generalized eigenvalues of the pencil  $(ZZ^\top + I, D + I)$ . Applying Lemma A.1 leads to the simple solution:  $ZZ^\top = \sum_{i=1}^r \delta_i^2 e_i e_i^\top$ , where  $(e_i)$  are the columns of the identity matrix. In particular, the solution is unique if the first  $r$  eigenvalues of  $S_{\text{pr}}^\top H S_{\text{pr}}$  are distinct. The corresponding approximation  $UU^\top$  is then

$$UU^\top = S_{\text{pr}}^{-\top} W Z Z^\top W^\top S_{\text{pr}}^{-1} = \sum_{i=1}^r \delta_i^2 \widetilde{w}_i \widetilde{w}_i^\top, \quad (\text{A.8})$$

where  $\widetilde{w}_i = S_{\text{pr}}^{-\top} w_i$  and  $w_i$  is the  $i$ th column of  $W$ . Woodbury's identity gives the corresponding negative update of  $\Gamma_{\text{pr}}$  as:

$$\widehat{\Gamma}_{\text{pos}} = \Gamma_{\text{pr}} - K K^\top, \quad K K^\top = \sum_{i=1}^r \delta_i^2 (1 + \delta_i^2)^{-1} \widehat{w}_i \widehat{w}_i^\top \quad (\text{A.9})$$

with  $\widehat{w}_i = S_{\text{pr}} w_i$ . At optimality,  $\sigma_i = 1$  for  $i \leq r$  and  $\sigma_i = (1 + \delta_i^2)^{-1}$  for  $i > r$ , proving (2.10).  $\square$

Before proving Lemma 2.2, we recall that the Kullback-Leibler (K-L) divergence and the Hellinger distance between two multivariate Gaussians,  $\nu_1 = \mathcal{N}(\mu, \Sigma_1)$  and  $\nu_2 = \mathcal{N}(\mu, \Sigma_2)$ , with the same mean and full rank covariance matrices are given, respectively, by [29]:

$$D_{\text{KL}}(\nu_1 \| \nu_2) = \frac{1}{2} \left[ \text{trace}(\Sigma_2^{-1} \Sigma_1) - \text{rank}(\Sigma_1) - \ln \left( \frac{\det(\Sigma_1)}{\det(\Sigma_2)} \right) \right] \quad (\text{A.10})$$

$$d_{\text{Hell}}(\nu_1, \nu_2) = \sqrt{1 - \frac{|\Sigma_1|^{1/4} |\Sigma_2|^{1/4}}{|\frac{1}{2}\Sigma_1 + \frac{1}{2}\Sigma_2|^{1/2}}}. \quad (\text{A.11})$$

**Proof of Lemma 2.2.** By (A.10), the K-L divergence between the posterior  $\nu_{\text{pos}}(y)$  and the Gaussian approximation  $\widehat{\nu}_{\text{pos}}(y)$  can be written in terms of the generalized eigenvalues of the pencil  $(\Gamma_{\text{pos}}, \widehat{\Gamma}_{\text{pos}})$  as:

$$D_{\text{KL}}(\nu_{\text{pos}}(y) \| \widehat{\nu}_{\text{pos}}(y)) = \sum_i (\sigma_i - \ln \sigma_i - 1) / 2,$$

and since  $f(x) = (x - \ln x - 1) / 2$  belongs to  $\mathcal{U}$ , we see that the K-L divergence is a loss function in the class  $\mathcal{L}$  defined by (2.6). Hence, Theorem 2.3 applies and the equivalence between the two approximations follows trivially. An analogous argument holds for the Hellinger distance. The squared Hellinger distance between  $\nu_{\text{pos}}(y)$  and  $\widehat{\nu}_{\text{pos}}(y)$  can be written in terms of the generalized eigenvalues,  $(\sigma_i)$ , of the pencil  $(\Gamma_{\text{pos}}, \widehat{\Gamma}_{\text{pos}})$ , as:

$$d_{\text{Hell}}(\nu_{\text{pos}}(y), \widehat{\nu}_{\text{pos}}(y))^2 = 1 - 2^{1/2} \prod_i \sigma_i^{1/4} (1 + \sigma_i)^{-1/2}. \quad (\text{A.12})$$

Minimizing (A.12) is equivalent to maximizing  $\prod_i \sigma_i^{1/4} (1 + \sigma_i)^{-1/2}$ , which in turn is equivalent to minimizing the functional:

$$L(\Gamma_{\text{pos}}, \hat{\Gamma}_{\text{pos}}) = - \sum_i \ln(\sigma_i^{1/4} (1 + \sigma_i)^{-1/2}) = \sum_i \ln(2 + \sigma_i + 1/\sigma_i)/4 \quad (\text{A.13})$$

Since  $f(x) = \ln(2 + x + 1/x)/4$  belongs to  $\mathcal{U}$ , Theorem 2.3 can be applied once again.  $\square$

**Proof of Corollary 3.1.** The proofs of parts (i) and (ii) were already given in the proof of Theorem 2.3. Part (iii) holds because,

$$\begin{aligned} (1 + \delta_i^2) \Gamma_{\text{pos}} \tilde{w}_i &= (1 + \delta_i^2) (H + \Gamma_{\text{pr}}^{-1})^{-1} S_{\text{pr}}^{-\top} w_i \\ &= (1 + \delta_i^2) S_{\text{pr}} (S_{\text{pr}}^\top H S_{\text{pr}} + I)^{-1} w_i = S_{\text{pr}} w_i = \Gamma_{\text{pr}} \tilde{w}_i, \end{aligned}$$

because  $w_i$  is an eigenvector of  $(S_{\text{pr}}^\top H S_{\text{pr}} + I)^{-1}$  with eigenvalue  $(1 + \delta_i^2)^{-1}$ .  $\square$

Now we turn to optimality results for approximations of the posterior mean. In what follows, let  $S_{\text{pr}}$ ,  $S_{\text{obs}}$ ,  $S_{\text{pos}}$ , and  $S_y$  be the matrix square roots of, respectively,  $\Gamma_{\text{pr}}$ ,  $\Gamma_{\text{obs}}$ ,  $\Gamma_{\text{pos}}$ , and  $\Gamma_y := \Gamma_{\text{obs}} + G \Gamma_{\text{pr}} G^\top$  such that  $\Gamma = S S^\top$  (i.e., possibly non-symmetric square roots).

Equation (4.1) shows that, to minimize  $\mathbb{E}(\|Ay - x\|_{\Gamma_{\text{pos}}^{-1}}^2)$  over  $A \in \mathcal{A}$ , we need only to minimize  $\mathbb{E}(\|Ay - \mu_{\text{pos}}(y)\|_{\Gamma_{\text{pos}}^{-1}}^2)$ . Furthermore, since  $\mu_{\text{pos}}(y) = \Gamma_{\text{pos}} G^\top \Gamma_{\text{obs}}^{-1} y$ , it follows that

$$\mathbb{E}(\|Ay - \mu_{\text{pos}}(y)\|_{\Gamma_{\text{pos}}^{-1}}^2) = \|S_{\text{pos}}^{-1} (A - \Gamma_{\text{pos}} G^\top \Gamma_{\text{obs}}^{-1}) S_y\|_F^2, \quad (\text{A.14})$$

We are therefore led to the following optimization problem:

$$\min_{A \in \mathcal{A}} \|S_{\text{pos}}^{-1} A S_y - S_{\text{pos}}^\top G^\top \Gamma_{\text{obs}}^{-1} S_y\|_F. \quad (\text{A.15})$$

The following result shows that the square root,  $S_{\hat{H}} = S_{\text{pr}}^\top G^\top S_{\text{obs}}^{-\top}$ , of  $\hat{H}$  (2.8) can be used to obtain simple expressions for the square roots of  $\Gamma_{\text{pos}}$  and  $\Gamma_y$ .

LEMMA A.3 (Square roots). *Let  $W D V^\top$  be an SVD of  $S_{\hat{H}} = S_{\text{pr}}^\top G^\top S_{\text{obs}}^{-\top}$ . Then:*

$$S_{\text{pos}} = S_{\text{pr}} W (I + D D^\top)^{-1/2} W^\top \quad (\text{A.16})$$

$$S_y = S_{\text{obs}} V (I + D^\top D)^{1/2} V^\top \quad (\text{A.17})$$

are square roots of  $\Gamma_{\text{pos}}$  and  $\Gamma_y$ .

*Proof.* We can rewrite  $\Gamma_{\text{pos}} = (G^\top \Gamma_{\text{obs}}^{-1} G + \Gamma_{\text{pr}}^{-1})^{-1}$  as

$$\begin{aligned} \Gamma_{\text{pos}} &= S_{\text{pr}} (S_{\hat{H}} S_{\hat{H}}^\top + I)^{-1} S_{\text{pr}}^\top = S_{\text{pr}} W (D D^\top + I)^{-1} W^\top S_{\text{pr}}^\top \\ &= [S_{\text{pr}} W (D D^\top + I)^{-1/2} W^\top] [S_{\text{pr}} W (D D^\top + I)^{-1/2} W^\top]^\top, \end{aligned}$$

which proves (A.16). The proof of (A.17) follows similarly using:  $S_{\hat{H}}^\top S_{\hat{H}} = S_{\text{obs}}^{-1} G \Gamma_{\text{pr}} G^\top \Gamma_{\text{obs}}^{-1}$ .  $\square$

In the next two proofs we use  $(C)_r$  to denote a rank  $r$  approximation of the matrix  $C$  in the Frobenius norm.

**Proof of Theorem 4.1.** By [14, Theorem 2.1], an optimal  $A \in \mathcal{A}_r$  is given by:

$$A = S_{\text{pos}} (S_{\text{pos}}^\top G^\top \Gamma_{\text{obs}}^{-1} S_y)_r S_y^{-1}. \quad (\text{A.18})$$

Now, we need some computations to show that (A.18) is equivalent to (4.4). Using (A.16) and (A.17) we find  $S_{\text{pos}}^\top G^\top \Gamma_{\text{obs}}^{-1} S_y = W (I + D D^\top)^{-1/2} D (I + D^\top D)^{1/2} V^\top$ , and therefore  $(S_{\text{pos}}^\top G^\top \Gamma_{\text{obs}}^{-1} S_y)_r =$

$\sum_{i=1}^r \delta_i w_i v_i^\top$ . Inserting this back into (A.18) yields (4.4). The minimum Bayes risk is a straightforward computation for the optimal estimator (4.4) using (A.14).  $\square$

**Proof of Theorem 4.2.** Given  $A \in \hat{\mathcal{A}}_r$ , we can restate (A.15) as the problem of finding a matrix  $B$ , of rank at most  $r$ , that minimizes:

$$\| S_{\text{pos}}^{-1}(\Gamma_{\text{pr}} - \Gamma_{\text{pos}}) G^\top \Gamma_{\text{obs}}^{-1} S_y - S_{\text{pos}}^{-1} B (G^\top \Gamma_{\text{obs}}^{-1} S_y) \|_F \quad (\text{A.19})$$

such that  $A = (\Gamma_{\text{pr}} - B) G^\top \Gamma_{\text{obs}}^{-1}$ . By [14, Theorem 2.1], an optimal  $B$  is given by:

$$B = S_{\text{pos}}(S_{\text{pos}}^{-1}(\Gamma_{\text{pr}} - \Gamma_{\text{pos}}) G^\top \Gamma_{\text{obs}}^{-1} S_y)_r (G^\top \Gamma_{\text{obs}}^{-1} S_y)^\dagger \quad (\text{A.20})$$

where  $\dagger$  denotes the pseudo-inverse operator. A closer look at [14, Theorem 2.1] reveals that another minimizer of (A.19), itself not necessarily of minimum Frobenius norm, is given by:

$$B = S_{\text{pos}}(S_{\text{pos}}^{-1}(\Gamma_{\text{pr}} - \Gamma_{\text{pos}}) G^\top \Gamma_{\text{obs}}^{-1} S_y)_r (S_{\text{pr}}^\top G^\top \Gamma_{\text{obs}}^{-1} S_y)^\dagger S_{\text{pr}}^\top. \quad (\text{A.21})$$

By Lemma A.3,

$$\begin{aligned} S_{\text{pr}}^\top G^\top \Gamma_{\text{obs}}^{-1} S_y &= W[D(I + D^\top D)^{1/2}]V^\top \\ S_{\text{pos}}^{-1} \Gamma_{\text{pr}} G^\top \Gamma_{\text{obs}}^{-1} S_y &= W[(I + DD^\top)^{1/2} D(I + D^\top D)^{1/2}]V^\top \\ S_{\text{pos}}^{-1} \Gamma_{\text{pos}} G^\top \Gamma_{\text{obs}}^{-1} S_y &= W[(I + DD^\top)^{-1/2} D(I + D^\top D)^{1/2}]V^\top \end{aligned}$$

and therefore  $(S_{\text{pr}}^\top G^\top \Gamma_{\text{obs}}^{-1} S_y)^\dagger = \sum_{i=1}^q \delta_i^{-1} (1 + \delta_i^2)^{-1/2} v_i w_i^\top$  for  $q = \text{rank}(S_{\hat{H}})$ , whereas

$$(S_{\text{pos}}^{-1}(\Gamma_{\text{pr}} - \Gamma_{\text{pos}}) G^\top \Gamma_{\text{obs}}^{-1} S_y)_r = \sum_{i=1}^r \delta_i^3 w_i v_i^\top.$$

Inserting these expressions back into (A.21), we obtain:

$$B = S_{\text{pr}} \left( \sum_{i=1}^r \frac{\delta_i^2}{1 + \delta_i^2} w_i w_i^\top \right) S_{\text{pr}}^\top.$$

By definition,  $(\delta_i^2)$  are the eigenvalues of  $\hat{H}$ . Hence, by Theorem 2.3, we recognize the optimal approximation of  $\Gamma_{\text{pos}}$  as  $\hat{\Gamma}_{\text{pos}} = \Gamma_{\text{pr}} - B$ . Plugging this expression back into (A.21) gives (4.6). The minimum Bayes risk in (ii) follows readily using the optimal estimator given by (4.6) in (A.14).  $\square$

## REFERENCES

- [1] V. AKÇELIK, G. BIROS, O. GHATTAS, J. HILL, D. KEYES, AND B. VAN BLOEMEN WAANDERS, *Parallel algorithms for PDE-constrained optimization*, Parallel Processing for Scientific Computing, 20 (2006), p. 291.
- [2] T. BUI-THAN, C. BURSTEDDE, O. GHATTAS, J. MARTIN, G. STADLER, AND L. WILCOX, *Extreme-scale UQ for Bayesian inverse problems governed by PDEs*, in Proceedings of the International Conference on High Performance Computing, Networking, Storage and Analysis, IEEE Computer Society Press, 2012, p. 3.
- [3] T. BUI-THANH AND O. GHATTAS, *Analysis of the Hessian for inverse scattering problems: I. Inverse shape scattering of acoustic waves*, Inverse Problems, 28 (2012), p. 055001.
- [4] T. BUI-THANH, O. GHATTAS, AND D. HIGDON, *Adaptive Hessian-based nonstationary Gaussian process response surface method for probability density approximation with application to Bayesian solution of large-scale inverse problems*, SIAM Journal on Scientific Computing, 34 (2012), pp. A2837–A2871.
- [5] T. BUI-THANH, O. GHATTAS, J. MARTIN, AND G. STADLER, *A computational framework for infinite-dimensional Bayesian inverse problems part I: The linearized case, with application to global seismic inversion*, SIAM Journal on Scientific Computing, 35 (2013), pp. A2494–A2523.
- [6] B.P. CARLIN AND T.A. LOUIS, *Bayesian Methods for Data Analysis*, Chapman & Hall/CRC, 3rd ed., 2009.
- [7] R.A. CHRISTENSEN, *Plane Answers to Complex Questions: The Theory of Linear Models*, Springer-Verlag, 1987.

- [8] J. CHUNG AND M. CHUNG, *An efficient approach for computing optimal low-rank regularized inverse matrices*, arXiv:1404.1610, 2014.
- [9] J. CHUNG, M. CHUNG, AND D.P. O'LEARY, *Optimal regularized low rank inverse approximation*, Linear Algebra and Applications (to appear), (2014).
- [10] T. CUI, K. J. H. LAW, AND Y. M. MARZOUK, *Dimension-independent likelihood-informed MCMC*, arXiv preprint, (2014).
- [11] T. CUI, J. MARTIN, Y. MARZOUK, A. SOLONEN, AND A. SPANTINI, *Likelihood-informed dimension reduction for nonlinear inverse problems*, Inverse Problems, in press (2014). arXiv:1403.4680.
- [12] H.P. FLATH, L. WILCOX, V. AKÇELİK, J. HILL, B. VAN BLOEMEN WAANDERS, AND O. GHATTAS, *Fast algorithms for Bayesian uncertainty quantification in large-scale linear inverse problems based on low-rank partial Hessian approximations*, SIAM Journal on Scientific Computing, 33 (2011), pp. 407–432.
- [13] W. FÖRSTNER AND B. MOONEN, *A metric for covariance matrices*, in Geodesy-The Challenge of the 3rd Millennium, Springer, 2003, pp. 299–309.
- [14] S. FRIEDLAND AND A. TOROKHTI, *Generalized rank-constrained matrix approximations*, SIAM Journal on Matrix Analysis and Applications, 29 (2007), pp. 656–659.
- [15] G.H. GOLUB AND C.F. VAN LOAN, *Matrix Computations*, vol. 3, JHU Press, 2012.
- [16] N. HALKO, P. MARTINSSON, AND J.A. TROPP, *Finding structure with randomness: Probabilistic algorithms for constructing approximate matrix decompositions*, SIAM Review, 53 (2011), pp. 217–288.
- [17] J. HEIKKINEN, *Statistical Inversion Theory in X-ray Tomography*, master's thesis, Lappeenranta University of Technology, Finland, 2008.
- [18] Y. HUA AND W. LIU, *Generalized Karhunen-Loève transform*, IEEE Signal Processing Letters, 5 (1998), pp. 141–142.
- [19] W. JAMES AND C. STEIN, *Estimation with quadratic loss*, in Proceedings of the Fourth Berkeley Symposium on Mathematical Statistics and Probability, vol. 1, 1961, pp. 361–379.
- [20] E.L. LEHMANN AND G. CASELLA, *Theory of Point Estimation*, Springer-Verlag, 1998.
- [21] A.S. LEWIS, *Derivatives of spectral functions*, Mathematics of Operations Research, 21 (1996), pp. 576–588.
- [22] W. LI AND O. A. CIRPKA, *Efficient geostatistical inverse methods for structured and unstructured grids*, Water Resources Research, 42 (2006), p. W06402.
- [23] C. LIEBERMAN, K. FIDKOWSKI, K. WILLCOX, AND B. VAN BLOEMEN WAANDERS, *Hessian-based model reduction: large-scale inversion and prediction*, International Journal for Numerical Methods in Fluids, 71 (2013), pp. 135–150.
- [24] C. LIEBERMAN, K. WILLCOX, AND O. GHATTAS, *Parameter and state model reduction for large-scale statistical inverse problems*, SIAM Journal on Scientific Computing, 32 (2010), pp. 2523–2542.
- [25] F. LINDGREN, H. RUE, AND J. LINDSTRÖM, *An explicit link between Gaussian fields and Gaussian Markov random fields: the stochastic partial differential equation approach*, Journal of the Royal Statistical Society: Series B, 73 (2011), pp. 423–498.
- [26] D.V. LINDLEY AND A.F.M. SMITH, *Bayes estimates for the linear model*, Journal of the Royal Statistical Society. Series B, (1972), pp. 1–41.
- [27] J. MARTIN, L. WILCOX, C. BURSTEDDE, AND O. GHATTAS, *A stochastic Newton MCMC method for large-scale statistical inverse problems with application to seismic inversion*, SIAM Journal on Scientific Computing, 34 (2012), pp. A1460–A1487.
- [28] Y. MARZOUK AND H.N. NAJM, *Dimensionality reduction and polynomial chaos acceleration of Bayesian inference in inverse problems*, Journal of Computational Physics, 228 (2009), pp. 1862–1902.
- [29] L. PARDO, *Statistical Inference Based on Divergence Measures*, CRC Press, 2005.
- [30] G.W. STEWART, *The efficient generation of random orthogonal matrices with an application to condition estimators*, SIAM Journal on Numerical Analysis, 17 (1980), pp. 403–409.
- [31] A. M. STUART, *Inverse problems: a Bayesian perspective*, Acta Numerica, 19 (2010), pp. 451–559.